Accepted Manuscript

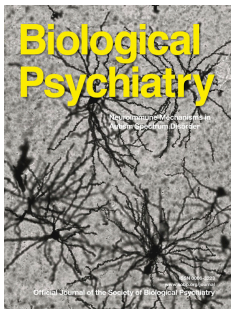

Mapping Cortical and Subcortical Asymmetry in Obsessive-Compulsive Disorder: Findings from the ENIGMA Consortium

Xiangzhen Kong, Premika S.W. Boedhoe, Yoshinari Abe, Pino Alonso, Stephanie H. Ameis, Paul D. Arnold, Francesca Assogna, Justin T. Baker, Marcelo C. Batistuzzo, Francesco Benedetti, Jan C. Beucke, Irene Bollettini, Anushree Bose, Silvia Brem, Brian P. Brennan, Jan Buitelaar, Rosa Calvo, Yuqi Cheng, Kang Ik K. Cho, Sara Dallaspezia, Damiaan Denys, Benjamin A. Ely, Jamie Feusner, Kate D. Fitzgerald, Jean-Paul Fouche, Egill A. Fridgeirsson, David C. Glahn, Patricia Gruner, Deniz A. Gürsel, Tobias U. Hauser, Yoshiyuki Hirano, Marcelo Q. Hoexter, Hao Hu, Chaim Huyser, Anthony James, Fern Jaspers-Fayer, Norbert Kathmann, Christian Kaufmann, Kathrin Koch, Masaru Kuno, Gerd Kvale, Jun Soo Kwon, Luisa Lazaro, Yanni Liu, Christine Lochner, Paulo Marques, Rachel Marsh, Ignacio Martínez-Zalacaín, David Mataix-Cols, Sarah E. Medland, José M. Menchón, Luciano Minuzzi, Pedro S. Moreira, Astrid Morer, Pedro Morgado, Akiko Nakagawa, Takashi Nakamae, Tomohiro Nakao, Janardhanan. C. Narayanaswamy, Erika L. Nurmi, Joseph O'Neill, Jose C. Pariente, Chris Perriello, John Piacentini, Fabrizio Piras, Federica Piras, Christopher Pittenger, Y.C. Janardhan Reddy, Oana Georgiana Rus-Oswald, Yuki Sakai, Joao R. Sato, Lianne Schmaal, H. Blair Simpson, Noam Soreni, Carles Soriano-Mas, Gianfranco Spalletta, Emily R. Stern, Michael C. Stevens, S. Evelyn Stewart, Philip R. Szeszko, David F. Tolin, Aki Tsuchiyagaito, Daan van Rooij, Guido A. van Wingen, Ganesan Venkatasubramanian, Zhen Wang, Je-Yeon Yun, ENIGMA-OCD Working Group, Paul M. Thompson, Dan J. Stein, Odile A. van den Heuvel, Clyde Francks

PII: S0006-3223(19)31292-2

DOI: https://doi.org/10.1016/j.biopsych.2019.04.022

Reference: BPS 13840

To appear in: *Biological Psychiatry*

Received Date: 20 November 2018

Revised Date: 21 March 2019

Accepted Date: 10 April 2019

Please cite this article as: Kong X., Boedhoe P.S.W., Abe Y., Alonso P., Ameis S.H., Arnold P.D., Assogna F., Baker J.T., Batistuzzo M.C., Benedetti F., Beucke J.C., Bollettini I., Bose A., Brem S., Brennan B.P., Buitelaar J., Calvo R., Cheng Y., Cho K.I.K., Dallaspezia S., Denys D., Ely B.A., Feusner J., Fitzgerald K.D., Fouche J.-P., Fridgeirsson E.A., Glahn D.C., Gruner P., Gürsel D.A., Hauser T.U., Hirano Y., Hoexter M.Q., Hu H., Huyser C., James A., Jaspers-Fayer F., Kathmann N., Kaufmann C., Koch K., Kuno M., Kvale G., Kwon J.S., Lazaro L., Liu Y., Lochner C., Marques P., Marsh R., Martínez-Zalacaín I., Mataix-Cols D., Medland S.E., Menchón J.M., Minuzzi L., Moreira P.S, Morer A., Morgado P., Nakagawa A., Nakamae T., Nakao T., Narayanaswamy J.C., Nurmi E.L., O'Neill J., Pariente J.C., Perriello C., Piacentini J., Piras F., Piras F., Pittenger C., Reddy Y.C.J., Rus-Oswald O.G., Sakai Y., Sato J.R., Schmaal L., Simpson H.B., Soreni N., Soriano-Mas C., Spalletta G., Stern E.R., Stevens M.C., Stewart S.E., Szeszko P.R., Tolin D.F., Tsuchiyagaito A., van Rooij D., van Wingen G.A., Venkatasubramanian G., Wang Z., Yun J.-Y., ENIGMA-OCD Working Group, Thompson P.M., Stein D.J., van den Heuvel O.A. & Francks C., Mapping Cortical and Subcortical Asymmetry in Obsessive-Compulsive Disorder: Findings from the ENIGMA Consortium, *Biological Psychiatry* (2019), doi: https://doi.org/10.1016/j.biopsych.2019.04.022.

Title: Mapping Cortical and Subcortical Asymmetry in Obsessive-Compulsive Disorder: Findings from the ENIGMA Consortium

Abbreviated title: Brain Asymmetry Alterations in OCD

Authors: Xiangzhen Kong (1), Premika S.W. Boedhoe (2,3), Yoshinari Abe (4), Pino Alonso (5,6,7), Stephanie H. Ameis (8,9), Paul D. Arnold (10,11), Francesca Assogna (12), Justin T. Baker (13), Marcelo C. Batistuzzo (14), Francesco Benedetti (15), Jan C. Beucke (16), Irene Bollettini (15), Anushree Bose (17), Silvia Brem (18,19), Brian P. Brennan (20), Jan Buitelaar (21), Rosa Calvo (22,23,24), Yuqi Cheng (25), Kang Ik K. Cho (26), Sara Dallaspezia (15), Damiaan Denys (27,28), Benjamin A. Ely (29), Jamie Feusner (30), Kate D. Fitzgerald (31), Jean-Paul Fouche (32,33), Egill A. Fridgeirsson (27), David C. Glahn (34,35), Patricia Gruner (36), Deniz A. Gürsel (37,38), Tobias U. Hauser (18,39,40), Yoshiyuki Hirano (41), Marcelo Q. Hoexter (14), Hao Hu (42), Chaim Huyser (43,44), Anthony James (45), Fern Jaspers-Fayer (46), Norbert Kathmann (16), Christian Kaufmann (16), Kathrin Koch (37,38), Masaru Kuno (41), Gerd Kvale (47,48), Jun Soo Kwon (49,50), Luisa Lazaro (22,51,23,24), Yanni Liu (31), Christine Lochner (52), Paulo Marques (53,54,55), Rachel Marsh (56,57), Ignacio Martínez-Zalacaín (5,7), David Mataix-Cols (58), Sarah E. Medland (59), José M. Menchón (5,6,7), Luciano Minuzzi (60), Pedro S Moreira (53,54,55), Astrid Morer (22,51,23,24), Pedro Morgado (53,54,55), Akiko Nakagawa (41), Takashi Nakamae (4), Tomohiro Nakao (61), Janardhanan. C. Narayanaswamy (17), Erika L. Nurmi (30), Joseph O'Neill (30), Jose C. Pariente (62), Chris Perriello (20,63), John Piacentini (30), Fabrizio Piras (12), Federica Piras (12), Christopher Pittenger (64), Y.C. Janardhan Reddy (17), Oana Georgiana Rus-Oswald (65), Yuki Sakai (66,4), Joao R. Sato (67), Lianne Schmaal (68,69), H. Blair Simpson (56,70), Noam Soreni (71), Carles Soriano-Mas (5,6,72), Gianfranco Spalletta (12,73), Emily R. Stern (74,75), Michael C. Stevens (76,77), S. Evelyn Stewart (78,79), Philip R. Szeszko (80,81), David F. Tolin (82,83), Aki Tsuchiyagaito (41,84), Daan van Rooij (21), Guido A. van Wingen (27), Ganesan Venkatasubramanian (17), Zhen Wang (42,85), Je-Yeon Yun (86,87), ENIGMA-OCD Working Group (88), Paul M. Thompson (89), Dan J. Stein (90), Odile A. van den Heuvel (2,3), Clyde Francks (1,91)

Affiliations:

1. Language and Genetics Department, Max Planck Institute for Psycholinguistics, Nijmegen, The Netherlands.

2. Amsterdam UMC, Vrije Universteit Amsterdam, Department of Psychiatry, Amsterdam Neuroscience, Amsterdam, The Netherlands.

3. Amsterdam UMC, Vrije Universiteit Amsterdam, Department of Anatomy & Neurosciences, Amsterdam Neuroscience, Amsterdam, The Netherlands.

4. Department of Psychiatry, Graduate School of Medical Science, Kyoto Prefectural University of Medicine, Kyoto, Japan.

5. Department of Psychiatry, Bellvitge University Hospital, Bellvitge Biomedical Research Institute-IDIBELL, L'Hospitalet de Llobregat, Barcelona, Spain.

6. Centro de Investigación Biomèdica en Red de Salud Mental-CIBERSAM, Barcelona, Spain.

7. Department of Clinical Sciences, University of Barcelona, Spain.

8. The Margaret and Wallace McCain Centre for Child, Youth & Family Mental Health, Campbell Family Mental Health Research Institute, The Centre for Addiction and Mental Health, Department of Psychiatry, Faculty of Medicine, University of Toronto, Toronto, Canada.

9. Centre for Brain and Mental Health, The Hospital for Sick Children, Toronto, Canada.

10. Mathison Centre for Mental Health Research & Education, Hotchkiss Brain Institute, Cumming School of Medicine, University of Calgary, Calgary, Alberta, Canada.

11. Department of Psychiatry, Cumming School of Medicine, University of Calgary, Calgary, Alberta, Canada.

12. Laboratory of Neuropsychiatry, Department of Clinical and Behavioral Neurology, IRCCS Santa Lucia Foundation, Rome, Italy.

13. McLean Hopsital, Harvard Medical School, Belmont, MA, U.S.A..

14. Departamento e Instituto de Psiquiatria do Hospital das Clinicas, IPQ HCFMUSP, Faculdade de Medicina, Universidade de Sao Paulo, SP, Brasil..

15. Psychiatry and Clinical Psychobiology, Division of Neuroscience, Scientific Institute Ospedale San Raffaele, Milano, Italy.

16. Department of Psychology, Humboldt-Universität zu Berlin, Berlin, Germany.

17. Obsessive-Compulsive Disorder (OCD) Clinic Department of Psychiatry National Institute of Mental Health & Neurosciences, Bangalore, India.

18. Department of Child and Adolescent Psychiatry and Psychotherapy, Psychiatric Hospital, University of Zurich, Zurich, Switzerland.

19. Neuroscience Center Zurich, University of Zurich and ETH Zurich, Zurich, Switzerland.

20. McLean Hospital, Harvard Medical School, Belmont, MA, U.S.A..

21. Department of Cognitive Neurosicence, Donders Institute for Brain, Cognition and Behavior, Radboudumc, Nijmegen, The Netherlands .

22. Department of Child and Adolescent Psychiatry and Psychology, Institute of Neurosciences, Hospital Clínic Universitari, Barcelona, Spain.

23. Department of Medicine, University of Barcelona, Barcelona, Spain.

24. Centro de Investigación Biomédica en red de Salud Mental (CIBERSAM), Spain.

25. Department of Psychiatry, First Affiliated Hospital of Kunming Medical University, Kunming, China.

26. Institute of Human Behavioral Medicine, SNU-MRC, Seoul, Republic of Korea.

27. Amsterdam UMC, University of Amsterdam, Department of Psychiatry, Amsterdam Neuroscience, Amsterdam, Netherlands.

28. Netherlands Institute for Neuroscience, Royal Netherlands Academy of Arts and Sciences, Amsterdam, The Netherlands.

29. Department of Neuroscience, Graduate School of Biomedical Sciences, Icahn School of Medicine at Mount Sinai, New York, NY, U.S.A.

30. Department of Psychiatry and Biobehavioral Sciences, University of California, Los Angeles, CA, U.S.A..

31. Department of Psychiatry, University of Michigan, Ann Arbor, Michigan, U.S.A..

32. Department of Psychiatry, University of Cape Town, Cape Town, South Africa.

33. Department of Psychiatry, University of Stellenbosch, Cape Town, South Africa.

34. Department of Psychiatry, Yale University School of Medicine, New Haven, CT, USA.

35. Olin Neuropsychiatric Research Center, Hartford, CT, USA.

36. Department of Psychiatry, Yale University School of Medicine, New Haven, Connecticut, U.S.A..

37. Department of Neuroradiology, Klinikum rechts der Isar, Technische Universität München, Germany.

38. TUM-Neuroimaging Center (TUM-NIC) of Klinikum rechts der Isar, Technische Universität München, Germany.

39. Max Planck UCL Centre for Computational Psychiatry and Ageing Research, London, UK.

40. Wellcome Centre for Human Neuroimaging, University College London, London, UK.

41. Research Center for Child Mental Development, Chiba University, Chiba, Japan.

42. Shanghai Mental Health Center Shanghai Jiao Tong University School of Medicine, PR China.

43. De Bascule, Academic Center for Child and Adolescent Psychiatry, Amsterdam, the Netherlands.

44. Department of child and adolescent psychiatry Amsterdam UMC, Amsterdam, The Netherlands.

45. Department of Psychiatry, Oxford University, Oxford, U.K..

46. University of British Columbia, Vancouver, BC, Canada.

47. OCD-team, Haukeland University Hospital, Bergen, Norway.

48. Department of Clinical Psychology, University of Bergen, Bergen, Norway.

49. Department of Psychiatry, Seoul National University College of Medicine, Seoul, Republic of Korea.

50. Department of Brain & Cognitive Sciences, Seoul National University College of Natural Sciences, Seoul, Korea.

51. Institut d'Investigacions Biomèdiques August Pi i Sunyer (IDIBAPS), Barcelona, Spain.

52. SU/UCT MRC Unit on Anxiety & Stress Disorders, Department of Psychiatry, University of Stellenbosch, South Africa.

53. Life and Health Sciences Research Institute (ICVS), School of Medicine, University of Minho, Braga, Portugal..

54. ICVS/3B's, PT Government Associate Laboratory, Braga/Guimarães, Portugal..

55. Clinical Academic Center-Braga, Braga, Portugal..

56. Columbia University Irving Medical Center, Columbia University, New York, NY, U.S.A..

57. The Division of Child and Adolescent Psychiatry, New York State Psychiatric Institute, Columbia University, New York, NY, U.S.A..

58. Department of Clinical Neuroscience, Centre for Psychiatry Research, Karolinska Institutet, Stockholm, Sweden.

59. Psychiatric Genetics, QIMR Berghofer Medical Research Institute, Brisbane, Queensland, Australia.

60. Mood Disorders Clinic, St. Joseph's HealthCare, Hamilton, Ontario, Canada.

61. Department of Neuropsychiatry, Graduate School of Medical Sciences, Kyushu University, Fukuoka, Japan.

62. Magnetic Resonance Image Core Facility, IDIBAPS (Institut d'Investigacions Biomèdiques August Pi i Sunyer), Barcelona, Spain.

63. University of Illinois at Urbana-Champaign, Champaign, IL, U.S.A..

64. Department of Psychiatry, Yale University School of Medicine, New Haven, Connecticut, U.S.A.

65. University of Zürich, University Hospital Zürich, Dept. Neuroradiology, Zürich, Germany.

66. ATR Brain Information Communication Research Laboratory Group, Kyoto, Japan.

67. Center of Mathematics, Computing and Cognition, Universidade Federal do ABC, Santo Andre, Brazil.

68. Orygen, The National Centre of Excellence in Youth Mental Health, Parkville, VIC, Australia.

69. Centre for Youth Mental Health, The University of Melbourne, Melbourne, VIC, Australia.

70. Center for OCD and Related Disorders, New York State Psychiatric Institute, New York, NY, U.S.A..

71. Pediatric OCD Consultation service, Anxiety Treatment and Research Center, St. Joseph's HealthCare, Hamilton, Ontario, Canada.

72. Department of Psychobiology and Methodology of Health Sciences, Universitat Autònoma de Barcelona, Spain.

73. Beth K. and Stuart C. Yudofsky Division of Neuropsychiatry, Department of Psychiatry and Behavioral Sciences, Baylor College of Medicine, Houston, Texas, USA.

74. Department of Psychiatry, New York University School of Medicine, New York, NY, U.S.A..

75. Nathan Kline Institute for Psychiatric Research, Orangeburg, NY, U.S.A..

76. Yale University School of Medicine, New Haven, Conneticut, U.S.A.

77. Clinical Neuroscience and Development Laboratory, Olin Neuropsychiatry Research Center, Hartford, Connecticut, U.S.A..

78. Department of Psychiatry, University of British Columbia, Vancouver, BC, Canada.

79. Provincial Obsessive-Compulsive Disorder Program, British Columbia Children's Hospital, Vancouver, BC, Canada.

80. Icahn School of Medicine at Mount Sinai, New York, U.S.A..

81. James J. Peters VA Medical Center, Bronx, New York, U.S.A.

82. Institute of Living/Hartford Hospital, Hartford, Connecticut, USA.

83. Yale University School of Medicine, New Haven, Connecticut, U.S.A.

84. Laureate Institute for Brain Research, Tulsa, Oklahoma, U.S.A.

85. Shanghai Key Laboratory of Psychotic Disorders, PR China.

86. Seoul National University Hospital, Seoul, Republic of Korea.

87. Yeongeon Student Support Center, Seoul national University College of Medicine, Seoul, Republic of Korea.

88. A complete list of the ENIGMA Laterality Working Group can be found in the SI document.

89. Imaging Genetics Center, Mark and Mary Stevens Neuroimaging & Informatics Institute, Keck School of Medicine of the University of Southern California, Marina del Rey, U.S.A..

90. SU/UCT MRC Unit on Risk & Resilience in Mental Disorders, Department of Psychiatry and Mental Health, University of Cape Town, South Africa.

91. Donders Institute for Brain, Cognition and Behavior, Radboud University, Nijmegen, The Netherlands.

Correspondence Author:

Clyde Francks, D.Phil. (Wundtlaan 1, 6525 XD Nijmegen, The Netherlands, +31-24-3521929, clyde.francks@mpi.nl)

Xiang-Zhen Kong, Ph.D. (Wundtlaan 1, 6525 XD Nijmegen, The Netherlands, +31-24-3521957, xiangzhen.kong@outlook.com)

Number of pages: 23

Number of Figures/Tables: 2/1

Number of words for Abstract: 229**; for Introduction:** 882**; for Discussion:** 1488

Total number of words: 3975

Number of supplementary material: 2 files (1 PDF with text and figures; 1 Excel with tables)

Abstract

Objective: Lateralized dysfunction has been suggested in Obsessive-Compulsive Disorder (OCD). However, it is currently unclear whether OCD is characterized by abnormal patterns of structural brain asymmetry. Here we carried out by far the largest study of brain structural asymmetry in OCD.

Method: We studied a collection of 16 pediatric datasets (501 OCD patients and 439 healthy controls), as well as 30 adult datasets (1777 patients and 1654 controls) from the OCD Working Group within the ENIGMA (Enhancing Neuro-Imaging Genetics through Meta-Analysis) consortium. Asymmetries of the volumes of subcortical structures, and of regional cortical thickness and surface area measures, were assessed based on T1-weighted MRI scans, using harmonized image analysis and quality control protocols. We investigated possible alterations of brain asymmetry in OCD patients. We also explored potential associations of asymmetry with specific aspects of the disorder and medication status.

Results: In the pediatric datasets, the largest case-control differences were observed for volume asymmetry of the thalamus (more leftward; Cohen's $d = 0.19$) and the pallidum (less leftward; $d = -0.21$). Additional analyses suggested putative links between these asymmetry patterns and medication status, OCD severity, and/or anxiety and depression comorbidities. No significant case-control differences were found in the adult datasets.

Conclusions: The results suggest subtle changes of the average asymmetry of subcortical structures in pediatric OCD, which are not detectable in adults with the disorder. These findings may reflect altered neurodevelopmental processes in OCD.

Keywords: laterality; brain asymmetry; obsessive-compulsive disorder; thalamus; pallidum; mega-analysis

Highlights:

Brain structural asymmetry alterations in patients with OCD were investigated.

This study was performed with a large sample size via the ENIGMA Consortium.

The largest case-control mean differences were found in the thalamus and pallidum in pediatric OCD patients.

Alterations of structural asymmetry in OCD were subtle and restricted to pediatric cases.

Introduction

Obsessive-Compulsive Disorder (OCD) is a psychiatric disorder with a lifetime prevalence of approximately 2% (1-4). OCD involves persistent, intrusive and unwanted thoughts (obsessions) as well as repetitive behaviors which might be accompanied by mental acts (compulsions) (4). As a heterogeneous neuropsychiatric condition with considerable heritability of roughly 40% (5), OCD has significant genetic and non-genetic determinants (4), but the pathophysiology of this complex disorder remains unclear.

Left-right asymmetry is an important aspect of human brain organization for multiple functions (6). For example visual-spatial processing and emotions that elicit withdrawal behaviors are usually right-lateralized in healthy people (7-10), whereas language-related processes, hand motor dominance, and emotions that elicit approach behaviors tend to be left-lateralized in the brain (11, 12). Alterations of asymmetry have been reported in various psychiatric and neurocognitive conditions, including schizophrenia (13, 14), autism (15) and dyslexia (16). Altered functional laterality has also been investigated in OCD (17, 18), partly due to observations of psychometric deficits within the visual-spatial domain (19-21), as well as altered emotional processing (22-25). For example, a behavioral study found reduced functional asymmetry for spatial attention in OCD patients, and also that less typical asymmetry was correlated with more serious obsessions (20). Several studies found greater impairment in visual-spatial memory compared with verbal memory in OCD, suggestive of right-sided dysfunction (17, 18, 26). Increased left-right asymmetry of electroencephalographic (EEG) activity at rest, or reduced activity in the right hemisphere linked to approach/avoidance motivation, has also been reported in OCD compared to healthy controls (19, 22). However, left-sided dysfunction has also been suggested in OCD, on the basis of neuropsychological data (23) as well as neuroimaging studies (27-29). Reduced right-ear advantage, which can indicate left-hemisphere dysfunction, was reported in OCD for certain tasks (23). In addition, hyper-responsiveness was observed in the left hemisphere based on event-related potentials (27, 30). More recently, left lateralized differences in functional connectivity of the amygdala were reported in OCD versus controls, using task fMRI (31). Studies with animal models of OCD (32), and transcranial magnetic stimulation (TMS) in treatment-resistant

OCD patients (33) have suggested that left-lateralized stimulation is more effective compared to right. Therefore, overall, the literature suggests altered hemispheric functional balance in OCD, but does not point consistently to one of the hemispheres as being the primary site of disruption.

Importantly, any structural basis linked to altered functional laterality in OCD is still unclear. Two previous studies explored brain structural asymmetry in OCD as a specific outcome of interest, but with low sample sizes. In one of these studies, with 16 OCD patients, leftward asymmetry (i.e., left > right) of cortical thickness in the anterior cingulate region was found in OCD patients and their siblings but not in matched controls, and this was claimed to present a potential endophenotype linked to increased hereditary risk for OCD (34). In the other study, with 32 patients, significant differences of frontal white matter volume asymmetry were found in both medicated (N = 19) and non-medicated (N = 13) patients, as compared with healthy controls (35). Unfortunately, small sample sizes tend to limit the reliability of findings in human neuroscience (36), and the extent of any association between OCD and structural brain asymmetry remains uncertain.

The OCD working group within the Enhancing Neuro-Imaging Genetics through Meta-Analysis (ENIGMA) consortium (37) recently achieved more highly powered analyses of brain changes in OCD, based on a sample size of over 1500 OCD individuals and a similar number of controls (38). They reported several regional case-control differences in cerebral cortical measures which involved only one hemisphere (38). However, these analyses did not examine whether effect sizes were significantly different on the left and right sides, and asymmetry was not quantitatively characterized. Unilateral patterns in this and other studies may arise from small but uniform bilateral effect sizes; the fact that statistical significance was achieved on one side, but not on the other, does not necessarily indicate a significant change in asymmetry. Furthermore, a post-hoc statistical comparison of the left and right-sided effect sizes as reported by the previous ENIGMA study (38) would not yield the same level of statistical power as can be provided by utilizing the individual-level, paired left and right data, to analyze asymmetry alterations in OCD. In addition, a previous ENIGMA study of subcortical volumes in OCD only reported combined left and right volumes (39).

Here, we used the latest data for both subcortical and cortical structures from the ENIGMA OCD Working Group, and targeted hemispheric structural asymmetry across subcortical and cortical measures, as assessed by subject-specific asymmetry indexes, AI = (Left-Right)/((Left+Right)/2) (40). The AI is a widely used approach in studies of brain asymmetry (e.g., (41, 42)). Our primary interest was to compare structural asymmetries between patients and healthy controls, but we also performed post-hoc analyses to investigate possible associations of brain asymmetries with medication status, age at disease onset, disease duration, OCD severity, and presence of anxiety and depression comorbidities. As the recent studies from the ENIGMA OCD working group had indicated distinct alterations in pediatric and adult patients (38, 39), and because asymmetries of both cortical and subcortical structures are also known to change subtly with age in the healthy population (40, 43), we carried out all analyses for the pediatric (<18 year old) and adult (>=18 year old) data separately (see also (44)).

Materials and Methods

See Supplementary Materials for detailed methods.

Datasets. The datasets used in this study were provided by members of the OCD Working Group within the ENIGMA Consortium (37). There were 46 independent datasets from 16 countries: 16 pediatric datasets comprising 501 OCD patients and 439 healthy controls, and 30 adult datasets comprising 1777 OCD patients and 1654 healthy controls (Table 1, Figure S1-2 and Table S1). All local institutional reviews boards permitted the use of extracted measures from their anonymized data. In addition, we leveraged publicly available summary statistics which describe the average form of brain regional asymmetries, based on our previous larger studies of healthy individuals (40, 43).

--Table 1--

Table 1. Information on participant numbers, age, sex and clinical characteristics in the ENIGMA OCD datasets.

Image Acquisition and Processing. Structural T1-weighted MRI scans were acquired and processed locally at each collection site. Images were acquired at different field strengths (1.5 T and 3T). All images were analyzed using one automated and validated pipeline, i.e. "recon-all" as implemented in *FreeSurfer*. For each subject, surface area and mean thickness was extracted for each of the 68 cortical regions (34 per hemisphere) in the Desikan-Killiany parcellation scheme (45), as well as total hemispheric surface area, and the average mean thickness over each hemisphere. In addition, volumes of eight subcortical regions of interest, including seven subcortical structures (nucleus accumbens, amygdala, caudate, hippocampus, pallidum, putamen, and thalamus), and the lateral ventricle volume, were calculated.

Asymmetry indexes. The aim of this study was to investigate differences in subcortical and cortical asymmetry related to OCD. To this end, for each participant, and each subcortical or cortical measure, an Asymmetry Index (AI) was defined as *(L-R)/((L+R)/2)*, where L and R represent the corresponding left and right volume measures (from subcortical regions), or thickness and surface area measures (from cortical regions). This AI formula has been widely used in previous brain asymmetry studies (41, 42, 46), including our own (8, 40, 43).

Case-control analyses. Separately for the pediatric and adult data, and for each AI, we pooled data from all available individuals from each dataset, and used a mega-analytical framework to investigate the case-control effects. Specifically, for each AI, we used a linear mixed-effect model (using *lme4* R package), with AI as the outcome variable, and a binary indicator of diagnosis (0=controls, 1=OCD patients) as the predictor of interest. In each model, a binary variable for sex, and a continuous measure for age (in years at time of scan) were included as confounding factors, and the categorical variable 'dataset' as a random-effect term.

Separately for thickness and surface area, we additionally calculated an overall 'typicality score' per subject, which indexed how much a given subject deviated from the population mean asymmetry profile, when considered simultaneously across all 34 cortical regions. A lower typicality score indicates more deviation from the mean asymmetry profile in the population.

OCD case-only analyses of clinical characteristics. For AIs which were potentially associated with OCD in the main analysis (see Results), we further investigated, within cases only, whether the AIs were associated with specific aspects of the disorder and medication status.

Results

An overview of the datasets is provided in Table 1, Figure S1-2, and Table S1.

Pediatric data. The results for both subcortical and cortical AIs in the pediatric data, including the effect size estimates for diagnosis on each AI, are presented in Figure 1 and Tables S2-S4.

The largest effects of diagnosis in pediatric cases were more leftward asymmetry of the thalamus (t = 2.84, p = 0.0047, d = 0.19; Figure 1-2), and less leftward asymmetry of the pallidum volume (t = -3.17, p = 0.0016, d = -0.21; Figure 1-2). These two findings were significant when controlling the FDR at 0.05 (see Materials and Methods). Post hoc analyses showed that these case-control differences were mainly due to a left thalamus which was relatively larger in OCD patients than controls (Left: t = 4.08, p = 4.89e-05, d = 0.27; Right: t = 2.12, p = 0.034, d = 0.14), and a left pallidum which was relatively smaller in OCD patients than controls (Left: t = -1.98, p = 0.048, d = -0.13; Right: t <1.0, p = 0.35, d = 0.062) (see also Figure 2B for distribution and group differences of each unilateral volume measure). In addition, we confirmed that the effects remained when excluding possible outliers in each AI per dataset (see Methods) (pediatric thalamus volume asymmetry: t = 2.90, p = 0.0038, d = 0.19; pediatric pallidum volume asymmetry: t = -3.16, p = 0.0016, d = -0.21).

<Fig. 1>

In terms of cortical asymmetries in the pediatric data, no significant case-control differences in the global hemispheric AI for either cortical thickness or surface area were found (ps >0.40). Regionally, only one AI showed a nominally significant effect (i.e. prior to multiple testing correction) of diagnosis, which was for thickness asymmetry of the lateral occipital cortex (greater rightward asymmetry in OCD patients; t = -2.08, p = 0.038, d = -0.14; Figure 2). This did not survive multiple

testing correction. No other AIs in case-control comparisons within the pediatric data showed significant effects (uncorrected *p*s >0.05).

<Fig. 2>

Within pediatric patients only, there were no differences of the thalamus or pallidum AIs between medicated and unmedicated subjects (uncorrected *p*s >0.20), nor with respect to current anxiety or depression comorbidity (*p*s >0.20), or age at disease onset or disease duration (*p*s >0.05). In terms of OCD symptom, the pallidum AI showed significant association with two of the 5 major Y-BOCS symptom components: hoarding (t = -2.37, p = 0.0065) and cleaning/contamination (t = -2.29, p = 0.014), such that cases with these symptoms had reduced leftward asymmetry of the pallidum compared to cases without these symptoms. No significant associations of symptom severity were observed with the thalamus AI, within the pediatric cases (*p*s >0.10).

When repeating the main analysis including age^2 in the model, in case of substantial non-linear effects of age on AIs, all of the Cohen's d for the effects of diagnosis remained within 0.005 of their values before having included age^2, and the same two AIs (thalamus volume AI, pallidum volume AI) remained significant after FDR correction. None of the AIs showed significant scanner effects in the pediatric data (*p*s >0.05), and the significant effects of diagnosis remained when adding scanner field strength as a predictor variable to the main analysis models (pediatric thalamus volume asymmetry: t = 2.81, p = 0.0050, d = 0.19; pediatric pallidum volume asymmetry: t = -3.02, p = 0.0025, d = -0.20).

We calculated per-subject 'typicality scores' (see Methods), and compared the typicality scores between patients and controls. However, no significant differences were found in the pediatric data for either thickness or surface area asymmetries (*p*s >0.15). This analysis might have been sensitive to multi-regional disruptions of laterality that are not consistent in direction, as could conceivably arise from generally increased developmental instability.

Adult data. The results for both subcortical and cortical AIs in the adult data, including the effect size estimates for diagnosis on each AI, are presented in Figure 1 and Tables S5-S7. All effects were subtle (Cohen's d between -0.086 and 0.066), and not as strong as found in the pediatric data.

The largest effect in adults was a case-control difference in the AI of global hemispheric surface area (t = -2.48, p = 0.013, d = -0.086), indicating that adult OCD was associated with slightly more rightward overall asymmetry in surface area, compared with controls. However, this did not survive multiple testing correction when accounting for all regional surface area AI comparisons. Post hoc analyses showed that this difference was mainly due to relatively smaller surface area in the left hemisphere (Left: t = -2.80, p = 0.0051, d = -0.098; Right: t = -2.18, p = 0.029, d = -0.076) in adult OCD patients than controls. The effect on this AI remained after excluding potential outliers (see Methods) (t = -3.03, p = 0.0025, d = -0.10). No significant case-control difference in the total average asymmetry of cortical thickness was found (p =0.35). No significant differences were found in regional asymmetries after multiple testing correction (Supplementary Materials).

Although the observed effect of diagnosis on the AI of global hemispheric surface area did not survive multiple testing correction, we were interested to explore associations of this AI with case-only variables, as it is a global rather than regional measure. Within the adult OCD patients, there was a trend towards unmedicated cases showing a mean AI difference compared to medicated cases (t = -1.77, p = 0.077, d =-0.086; i.e., more rightward asymmetry in medicated cases). Adult cases with current depression showed a mean AI difference compared to those without (t = -2.15, p = 0.032, d = -0.17; i.e., more rightward asymmetry in cases with current depression), while no effect of current anxiety comorbidity was observed (p =0.48). There was no correlation of this AI with the age at disease onset (t <1.0, p = 0.53) or the disease duration (t = -1.03, p =0.30). In terms of OCD severity measures, no significant associations were found with either the severity in total score or the subcomponent variables (ps >0.10).

Including age^2 or scanner field strength did not change the main results (Supplementary Materials). Typicality scores (see Methods) showed no case-control differences in the adult data, for either thickness or surface area asymmetry (ps >0.15).

The effect sizes of the AI case-control differences in the pediatric and adult data were found to be uncorrelated across the 34 cortical regions, for either thickness AIs or surface area AIs (ps >0.40).

Discussion

In this study we aimed to map differences in brain asymmetry between OCD patients and healthy controls, by leveraging a collection of 16 pediatric datasets and 30 adult datasets, via the ENIGMA Consortium. Using by far the largest sample size to address this issue to date, the results revealed a small number of asymmetry differences in OCD patients. The largest effects were in the pediatric patients for the volume asymmetry of the thalamus and the pallidum. These effects both had Cohen's *d* values of around 0.2, which indicates their subtlety and suggests that altered structural brain asymmetry alone is unlikely to be a clinically useful predictor of OCD. Nonetheless, these effect sizes were comparable to those reported by previous large-scale studies of disorder-related changes in brain structure, in which asymmetry was not studied, including studies of OCD as well as major depression, schizophrenia, and autism (e.g., (38, 39, 47-51)). Given that the effect sizes in the present study were estimated based on large sample sizes, relatively accurate estimations of the true effects were possible, whether they were statistically significant or not. As such, the effects are informative to share with the field.

Our finding of subtle changes in thalamus asymmetry in pediatric patients is broadly in accordance with previous disease models for OCD as regards the cortico-striato-thalamo-cortical (CSTC) circuitry, which is involved in a wide range of cognitive, motivational and emotional processes (44). Boedhoe *et al.* (39) observed a mean increase in bilateral thalamus volume (left plus right) in pediatric OCD patients versus controls, while in the present study, with a larger collection of 16 datasets (including 10 datasets used by Boedhoe *et al*.), we found that this OCD-related volume alteration was largely left-lateralized and resulted in altered thalamus asymmetry. It is not clear what pathophysiological mechanisms might link altered thalamus asymmetry to OCD. Within OCD individuals, we found no associations of thalamus asymmetry with medication status, age at a disease onset, disease duration, current anxiety and depression comorbidity, or disease symptoms, which might have given some insights into the observed differences. The thalamus is involved in diverse interactions among cortical, subcortical, and brainstem nuclei, and many of its functions are asymmetrical in normal subjects (52).

In addition, the thalamus is subdivided into cytoarchitectonically distinct nuclei with different functions (53). Future studies using higher resolution mapping of internal thalamus subsegments' structure and function may therefore be informative in pediatric OCD.

For the pallidum, no total volume change (left plus right) was reported by Boedhoe *et al*. in pediatric OCD patients, while here, with a larger collection of 16 pediatric datasets (including 10 used by Boedhoe *et al.*), we found an asymmetry difference of the pallidum which was largely driven by a significantly reduced left-sided volume in pediatric OCD patients. Boedhoe *et al.* also reported that adult OCD patients showed a larger pallidum (again left plus right) than controls, driven by patients with a childhood-onset of disease (39). We saw no significant effect on pallidum asymmetry in adult patients, in either the subgroups of early- or late-onset of disease (Supplemental Materials). This overall pattern of results suggests that disease chronicity, cumulative treatment effects and/or late adolescent volumetric changes in patients are linked to a bilateral increase in pallidum volume, but that reduced left sided volume in pediatric patients reflects a different, earlier developmental process. Moreover, pallidum asymmetry in the pediatric patients showed associations with symptom components "hoarding" and "cleaning/contamination". Although recently "hoarding disorder" was suggested as a separate diagnostic entity (54), in the present data there was only 1 case with hoarding behavior in the absence of other symptoms. Thus, we do not consider this tentative effect on asymmetry to relate to hoarding disorder specifically.

The pallidum, linking with the striatum and the thalamus within the CSTC circuitry (44), has roles in reward and motivation, as well as broader cognitive, affective and sensorimotor processes (44, 55). Further studies on specific functions of the (left) pallidum in compulsive symptoms, cleaning/contamination behaviors specifically, are needed. While it is not clear why lateralized changes in particular should be involved, in general terms our findings in pediatric cases help to characterize the brain structural changes in this disorder, and suggest altered subcortical neurodevelopment affecting the cortico-striato-thalamo-cortical circuitry. Further research will be needed to clarify any potential functional relevance of asymmetrical alterations in particular.

In terms of cortical measures in the pediatric data, we found no significant case-control differences in the asymmetry of regional or global measures of cortical thickness or surface area. This indicates that none of the cortical case-control differences reported by the previous large-scale ENIGMA study (38) are significantly lateralized, even when they might have been reported with respect to only one side. We also used a multivariable measure to describe the 'typicality' of each subject's asymmetry pattern over all cortical regions with respect to a healthy and general population database (40). However, no case-control differences in this measure were found. Together these analyses indicate that alterations of cerebral cortical anatomical asymmetry are not notable features of pediatric OCD.

In the adult data, there was no evidence for case-control differences of regional asymmetries, for either subcortical or cortical measures. The strongest cortical effect in adults was at the total hemispheric level, whereby cases showed slightly more rightward asymmetry of total surface area, mainly due to having a relatively smaller surface area in the left hemisphere than controls. However, this very small effect, with Cohen's *d* of 0.086, was not significant in the context of multiple testing, so that further studies with even larger sample sizes will be needed to confirm or refute this result. The effect was more pronounced in cases with comorbid depression, although this observation also remains tentative in the context of multiple testing.

Consistently with the previous findings of distinct alterations between pediatric and adult patients by the ENIGMA OCD Working Group (38, 39), the present study of structural asymmetry also showed different OCD-related effects between pediatric and adult data. There was also no correlation of case-control asymmetry differences between pediatric and adult data across the 34 cortical regions, which further supported the distinct OCD-related effects between pediatric and adult patients. Nonetheless, it is intriguing that the most notable effects in the pediatric and adult data all involved predominantly left-hemisphere alterations, which might support previous models of left-hemisphere dysfunction in OCD, as have been suggested by some functional imaging and neuropsychological findings (see Introduction) (23, 27-29). However, it will be important for future functional imaging studies to avoid reporting lateralized dysfunction on the basis that only one of the two hemispheres shows significant

case-control differences. This is because, as noted in the Introduction, a hemispheric difference of significance does not necessarily indicate a significant difference of effects between hemispheres.

OCD is a heterogeneous neuropsychiatric condition with a heritability of roughly 40%, as has been observed using both twin/family based estimation and SNP-based estimation (5, 56). A recent study showed that genetic variation across the genome, which impacts risk for OCD, also includes variation which affects the volumes of the nucleus accumbens and putamen (57). The structural brain asymmetries which showed the strongest associations with OCD in the present study have been shown to have significant heritability: 23% for the volume asymmetry of the thalamus, 15% for the volume asymmetry of the pallidum (43), and 17% for the total hemispheric asymmetry of cerebral cortical surface area (40). It may therefore be useful in future studies to assess the genetic correlation between these aspects of brain asymmetry and OCD, which might lead towards genome-wide association studies (58) to identify individual genetic loci that are involved in OCD-related asymmetry abnormalities.

This study has several limitations. First, the cross-sectional study design limits the interpretation of the results particularly with respect to age-related changes. Further work using longitudinal studies, and incorporating genetic and environmental variables, may be useful to understand the mechanisms underlying the potential associations reported here. Second, while the region-based approach used in this study is feasible for large-scale, collaborative projects, it is necessarily limited in terms of spatial resolution, and this might have contributed to some of the null results for regional cortical or subcortical regions. Investigation with more fined definition of regions (e.g., sub-regions of the thalamus (59)) or a vertex-wise approach combined with cross-hemispheric registration methods will be likely to be useful for future cortical asymmetry studies (60, 61). Third, the symptoms of OCD are heterogeneous (4). Identifying potential subtypes of OCD could therefore provide further insights into the pathophysiology.

In summary, we mapped structural brain asymmetry in pediatric and adult OCD as compared to controls, using by far the largest sample size to date. Effects were small overall, and most pronounced in the thalamus and the pallidum in pediatric patients, which also showed potential links with

medication status, disorder severity, and/or anxiety and depression comorbidities. Our study adds to literature implicating the thalamus in the pathophysiology of pediatric OCD, and additionally implicates the pallidum in pediatric cases. The full set of results from this study is available in the SI Tables and online for easy access (https://conxz.github.io/AsymOCD/).

Acknowledgments

The ENIGMA-OCD Working Group. Xiangzhen Kong (1), Premika S.W. Boedhoe (2,3), Yoshinari Abe (4), Pino Alonso (5,6,7), Stephanie H. Ameis (8,9), Alan Anticevic (10), Paul D. Arnold (11,12), Francesca Assogna (13), Justin T. Baker (14), Nerisa Banaj (13), Nuria Bargalló (15,16), Marcelo C. Batistuzzo (17), Francesco Benedetti (18), Jan C. Beucke (19), Irene Bollettini (18), Anushree Bose (20), Daniel Brandeis (21,22), Silvia Brem (23,24), Brian P. Brennan (25), Jan Buitelaar (26), Geraldo F. Busatto (17), Anna Calvo (15), Rosa Calvo (27,28,29), Yuqi Cheng (30), Kang Ik K. Cho (31), Valentina Ciullo (13,32), Sara Dallaspezia (18), Damiaan Denys (33,34), Froukje E. de Vries (2), Stella J. de Wit (2), Erin Dickie (35), Renate Drechsler (21), Benjamin A. Ely (36), Madalena Esteves (37,38,39), Andrea Falini (40), Yu Fang (41), Jamie Feusner (42), Martijn Figee (43,33), Kate D. Fitzgerald (41), Martine Fontaine (44), Jean-Paul Fouche (45,46), Egill A. Fridgeirsson (33), Patricia Gruner (10), Deniz A. Gürsel (47,48), Geoff Hall (49), Sayo Hamatani (50), Gregory L. Hanna (41), Bjarne Hansen (51,52), Tobias U. Hauser (23,53,54), Yoshiyuki Hirano (50), Marcelo Q. Hoexter (17), Hao Hu (55), Chaim Huyser (56,57), Keisuke Ikari (58), Neda Jahanshad (59), Anthony James (60), Fern Jaspers-Fayer (61), Norbert Kathmann (19), Christian Kaufmann (19), Kathrin Koch (47,48), Masaru Kuno (50), Gerd Kvale (51,52), Jun Soo Kwon (62,63), Luisa Lazaro (27,64,28,29), Yanni Liu (41), Christine Lochner (65), Ricardo Magalhães (37,38,39), Paulo Marques (37,38,39), Rachel Marsh (44,66), Ignacio Martínez-Zalacaín (5,7), Yasutaka Masuda (67), David Mataix-Cols (68), Koji Matsumoto (67), James T. McCracken (42), José M. Menchón (5,6,7), Euripedes C. Miguel (17), Luciano Minuzzi (69), Pedro S Moreira (37,38,39), Astrid Morer (27,64,28,29), Pedro Morgado (37,38,39), Akiko Nakagawa (50), Takashi Nakamae (4), Tomohiro Nakao (58), Janardhanan. C. Narayanaswamy (20), Jin Narumoto (4), Seiji Nishida (4), Erika L. Nurmi (42), Joseph O'Neill (42), Jose C. Pariente (15), Chris Perriello (25,70), John Piacentini (42), Fabrizio Piras (13), Federica Piras (13), Christopher Pittenger (71), Sara Poletti (18), Y.C. Janardhan Reddy (20), Tim Reess (47,48), Oana Georgiana Rus-Oswald (72), Yuki Sakai (73,4), Joao R. Sato (74), Lianne Schmaal (75,76), Eiji Shimizu (50,77), H. Blair Simpson (44,78), Noam Soreni (79), Carles Soriano-Mas (5,6,80), Nuno Sousa (37,38,39), Gianfranco Spalletta (13,81), Emily R. Stern (82,83), Michael C. Stevens (84,85), S. Evelyn Stewart (86,87), Philip R. Szeszko (88,89), Jumpei Takahashi (50), Jinsong Tang (42), Anders Lillevik Thorsen (51,52,90), David F. Tolin (91,92), Aki Tsuchiyagaito (50,93), Daan van Rooij (26), Guido A. van Wingen (33), Ysbrand D. van der Werf (3), Dick J. Veltman (2), Daniela Vecchio (13), Ganesan Venkatasubramanian (20), Susanne Walitza (21), Zhen Wang (55,94), Anri Watanabe (4), Jian Xu (95), Xiufeng Xu (30), Kei Yamada (96), Tokiko Yoshida (50), Je-Yeon Yun (97,98), Mojtaba Zarei (99), Qing Zhao (55), Cong Zhou (30), Paul M. Thompson (100), Dan J. Stein (101), Odile A. van den Heuvel (2,3), Clyde Francks (1,102)

1. Language and Genetics Department, Max Planck Institute for Psycholinguistics, Nijmegen, The Netherlands; 2. Amsterdam UMC, Vrije Universteit Amsterdam, Department of Psychiatry, Amsterdam Neuroscience, Amsterdam, The Netherlands; 3. Amsterdam UMC, Vrije Universiteit Amsterdam, Department of Anatomy & Neurosciences, Amsterdam Neuroscience, Amsterdam, The Netherlands; 4. Department of Psychiatry, Graduate School of Medical Science, Kyoto Prefectural University of Medicine, Kyoto, Japan; 5. Department of Psychiatry, Bellvitge University Hospital, Bellvitge Biomedical Research Institute-IDIBELL, L'Hospitalet de Llobregat, Barcelona, Spain; 6. Centro de Investigación Biomèdica en Red de Salud Mental-CIBERSAM, Barcelona, Spain; 7. Department of Clinical Sciences, University of Barcelona, Spain; 8. The Margaret and Wallace McCain Centre for Child, Youth & Family Mental Health, Campbell Family Mental Health Research Institute, The Centre for Addiction and Mental Health, Department of Psychiatry, Faculty of Medicine, University of Toronto, Toronto, Canada; 9. Centre for Brain and Mental Health, The Hospital for Sick Children, Toronto, Canada; 10. Department of Psychiatry, Yale University School of Medicine, New Haven, Connecticut, U.S.A.; 11. Mathison Centre for Mental Health Research & Education, Hotchkiss Brain Institute, Cumming School of Medicine, University of Calgary, Calgary, Alberta, Canada; 12. Department of Psychiatry, Cumming School of Medicine, University of Calgary, Calgary, Alberta, Canada; 13. Laboratory of Neuropsychiatry, Department of Clinical and Behavioral Neurology, IRCCS Santa Lucia Foundation, Rome, Italy; 14. McLean Hopsital, Harvard Medical School, Belmont, MA, U.S.A.; 15. Magnetic Resonance Image Core Facility, IDIBAPS (Institut d'Investigacions Biomèdiques August Pi i Sunyer), Barcelona, Spain; 16. Image Diagnostic Center, Hospital Clínic, Barcelona, Spain; 17. Departamento e Instituto de Psiquiatria do Hospital das Clinicas, IPQ HCFMUSP, Faculdade de Medicina, Universidade de Sao Paulo, SP, Brasil.; 18. Psychiatry and Clinical Psychobiology, Division of Neuroscience, Scientific Institute Ospedale San Raffaele, Milano, Italy; 19. Department of Psychology, Humboldt-Universität zu Berlin, Berlin, Germany; 20. Obsessive-Compulsive Disorder (OCD) Clinic Department of Psychiatry National Institute of Mental Health & Neurosciences, Bangalore, India; 21. Department of Child and Adolescent Psychiatry and Psychotherapy, Psychiatric Hospital, University of Zurich, Zurich Switzerland; 22. Department of Child and Adolescent Psychiatry and Psychotherapy, Central Institute of Mental Health, Medical Faculty, Mannheim, Heidelberg University, Mannheim, Germany; 23. Department of Child and Adolescent Psychiatry and Psychotherapy, Psychiatric Hospital, University of Zurich, Zurich, Switzerland; 24. Neuroscience Center Zurich, University of Zurich and ETH Zurich, Zurich, Switzerland; 25. McLean Hospital, Harvard Medical School, Belmont, MA, U.S.A.; 26. Department of Cognitive Neurosicence, Donders Institute for Brain, Cognition and Behavior, Radboudumc, Nijmegen, The Netherlands ; 27. Department of Child and Adolescent Psychiatry and Psychology, Institute of Neurosciences, Hospital Clínic Universitari, Barcelona, Spain; 28. Department of Medicine, University of Barcelona, Barcelona, Spain; 29. Centro de Investigación Biomédica en red de Salud Mental (CIBERSAM), Spain; 30. Department of Psychiatry, First Affiliated Hospital of Kunming Medical University, Kunming, China; 31. Institute of Human Behavioral Medicine, SNU-MRC, Seoul, Republic of Korea; 32. Department of Neurosciences, Psychology, Drug Research and Child Health (NEUROFARBA), University of Florence, Italy; 33. Amsterdam UMC, University of Amsterdam, Department of Psychiatry, Amsterdam Neuroscience, Amsterdam,

Netherlands; 34. Netherlands Institute for Neuroscience, Royal Netherlands Academy of Arts and Sciences, Amsterdam, The Netherlands; 35. Campbell Family Mental Health Research Institute, The Centre for Addiction and Mental Health, Department of Psychiatry, Faculty of Medicine, University of Toronto, Toronto, Canada; 36. Department of Neuroscience, Graduate School of Biomedical Sciences, Icahn School of Medicine at Mount Sinai, New York, NY, U.S.A; 37. Life and Health Sciences Research Institute (ICVS), School of Medicine, University of Minho, Braga, Portugal.; 38. ICVS/3B's, PT Government Associate Laboratory, Braga/Guimarães, Portugal.; 39. Clinical Academic Center-Braga, Braga, Portugal.; 40. Neuroradiology, Division of Neuroscience, Scientific Institute Ospedale San Raffaele, Milano, Italy; 41. Department of Psychiatry, University of Michigan, Ann Arbor, Michigan, U.S.A.; 42. Department of Psychiatry and Biobehavioral Sciences, University of California, Los Angeles, CA, U.S.A.; 43. Department of Psychiatry, Icahn School of Medicine at Mount Sinai, New York, USA.; 44. Columbia University Irving Medical Center, Columbia University, New York, NY, U.S.A.; 45. Department of Psychiatry, University of Cape Town, Cape Town, South Africa; 46. Department of Psychiatry, University of Stellenbosch, Cape Town, South Africa; 47. Department of Neuroradiology, Klinikum rechts der Isar, Technische Universität München, Germany; 48. TUM-Neuroimaging Center (TUM-NIC) of Klinikum rechts der Isar, Technische Universität München, Germany; 49. Department of Psychology, McMster University, Hamilton, Ontario, Canada; 50. Research Center for Child Mental Development, Chiba University, Chiba, Japan; 51. OCD-team, Haukeland University Hospital, Bergen, Norway; 52. Department of Clinical Psychology, University of Bergen, Bergen, Norway; 53. Max Planck UCL Centre for Computational Psychiatry and Ageing Research, London, UK; 54. Wellcome Centre for Human Neuroimaging, University College London, London, UK; 55. Shanghai Mental Health Center Shanghai Jiao Tong University School of Medicine, PR China; 56. De Bascule, Academic Center for Child and Adolescent Psychiatry, Amsterdam, the Netherlands; 57. Department of child and adolescent psychiatry Amsterdam UMC, Amsterdam, The Netherlands; 58. Department of Neuropsychiatry, Graduate School of Medical Sciences, Kyushu University, Fukuoka, Japan; 59. Imaging Genetics Center, Mark and Mary Stevens Neuroimaging and Informatics Institute, Keck School of Medicine of USC, Marina del Rey, CA 90292 USA; 60. Department of Psychiatry, Oxford University, Oxford, U.K.; 61. University of British Columbia, Vancouver, BC, Canada; 62. Department of Psychiatry, Seoul National University College of Medicine, Seoul, Republic of Korea; 63. Department of Brain & Cognitive Sciences, Seoul National University College of Natural Sciences, Seoul, Korea; 64. Institut d'Investigacions Biomèdiques August Pi i Sunyer (IDIBAPS), Barcelona, Spain; 65. SU/UCT MRC Unit on Anxiety & Stress Disorders, Department of Psychiatry, University of Stellenbosch, South Africa; 66. The Division of Child and Adolescent Psychiatry, New York State Psychiatric Institute, Columbia University, New York, NY, U.S.A.; 67. Department of Radiology, Chiba University Hospital, Chiba, Japan; 68. Department of Clinical Neuroscience, Centre for Psychiatry Research, Karolinska Institutet, Stockholm, Sweden; 69. Mood Disorders Clinic, St. Joseph's HealthCare, Hamilton, Ontario, Canada; 70. University of Illinois at Urbana-Champaign, Champaign, IL, U.S.A.; 71. Department of Psychiatry, Yale University School of Medicine, New Haven, Connecticut, U.S.A; 72. University of Zürich, University Hospital Zürich, Dept. Neuroradiology, Zürich, Germany; 73. ATR Brain Information Communication Research Laboratory Group, Kyoto, Japan; 74. Center of Mathematics, Computing and Cognition, Universidade Federal do ABC, Santo Andre, Brazil; 75. Orygen, The National Centre of Excellence in Youth Mental Health, Parkville, VIC, Australia; 76. Centre for Youth Mental Health, The University of Melbourne, Melbourne, VIC, Australia; 77. Department of Cognitive Behavioral Physiology, Graduate School of Medicine, Chiba University, Chiba, Japan; 78. Center for OCD and Related Disorders, New York State Psychiatric Institute, New York, NY, U.S.A.; 79. Pediatric OCD Consultation service, Anxiety Treatment and Research Center, St. Joseph's HealthCare, Hamilton, Ontario, Canada; 80. Department of Psychobiology and Methodology of Health Sciences, Universitat Autònoma de Barcelona, Spain; 81. Beth K. and Stuart C. Yudofsky Division of Neuropsychiatry, Department of Psychiatry and Behavioral Sciences, Baylor College of Medicine, Houston, Texas, USA; 82. Department of Psychiatry, New York University School of Medicine, New York, NY, U.S.A.; 83. Nathan Kline Institute for Psychiatric Research, Orangeburg, NY, U.S.A.; 84. Yale University School of Medicine, New Haven, Conneticut, U.S.A; 85. Clinical Neuroscience and Development Laboratory, Olin Neuropsychiatry Research Center, Hartford, Connecticut, U.S.A.; 86. Department of Psychiatry, University of British Columbia, Vancouver, BC, Canada; 87. Provincial Obsessive-Compulsive Disorder Program, British Columbia Children's Hospital, Vancouver, BC, Canada; 88. Icahn School of Medicine at Mount Sinai, New York, U.S.A.; 89. James J. Peters VA Medical Center, Bronx, New York, U.S.A; 90. Department of Anatomy and Neurosciences, Amsterdam UMC, Amsterdam, The Netherlands; 91. Institute of Living/Hartford Hospital, Hartford, Connecticut, USA; 92. Yale University School of Medicine, New Haven, Connecticut, U.S.A; 93. Laureate Institute for Brain Research, Tulsa, Oklahoma, U.S.A; 94. Shanghai Key Laboratory of Psychotic Disorders, PR China; 95. Department of Internal Medicine, First Affiliated Hospital of Kunming Medical University, Kunming, China; 96. Department of Radiology, Graduate School of Medical Science Kyoto Prefectural University of Medicine, Kyoto, Japan; 97. Seoul National University Hospital, Seoul, Republic of Korea; 98. Yeongeon Student Support Center, Seoul national University College of Medicine, Seoul, Republic of Korea; 99. Institute of Medical Science and Technology, Shahid Beheshti University, Tehran, Iran ; 100. Imaging Genetics Center, Mark and Mary Stevens Neuroimaging & Informatics Institute, Keck School of Medicine of the University of Southern California, Marina del Rey, U.S.A.; 101. SU/UCT MRC Unit on Risk & Resilience in Mental Disorders, Department of Psychiatry and Mental Health, University of Cape Town, South Africa; 102. Donders Institute for Brain, Cognition and Behavior, Radboud University, Nijmegen, The Netherlands

Yoshinari Abe was supported by JSPS KAKENHI Grant Numbeer 18K15523; Pino Alonso was supported by Project grant PI14/00419 from the Carlos III Health Institute. ; Stephanie H. Ameis was supported by funding for this project from an Ontario Mental Health Foundation Research Training Fellowship; Paul D. Arnold was supported by Funding for this project from Alberta Innovates Translational Health Chair in Child and Youth Mental Health and the Ontario Brain Institute; Justin T.

Baker was supported by NIMH K23MH104515; Marcelo C. Batistuzzo was supported by Fundação de Amparo à Pesquisa do Estado de São Paulo (FAPESP, São Paulo Research Foundation; Grant no. 2011/21357-9); Silvia Brem was supported by the Swiss National Science Foundation Grant (no. 320030_130237, principal investigator: Susanne Walitza) and the Hartmann Müller Foundation (no. 1460); Brian P. Brennan was supported by Grant K23-MH092397 from the National Institute of Mental Health (BPB) and the David Judah Fund at the Massachusetts General Hospital (BPB). Grant K23-MH104515 from the National Institute of Mental Health (JTB); Jan Buitelaar was supported by EU FP7 project TACTICS (grant nr 278948); Geraldo F. Busatto was supported by Fundação de Amparo à Pesquisa do Estado de São Paulo (FAPESP, São Paulo Research Foundation; Grant no. 2011/21357-9); Yuqi Cheng was supported by the National Natural Science Foundation of China (81560233); Kate D. Fitzgerald was supported by NIMH K23MH082176; Patricia Gruner was supported by IOCDF Award and K23 MH115206; Tobias U. Hauser was supported by a Wellcome Sir Henry Dale Fellowship (211155/Z/18/Z), a grant from the Jacobs Foundation, and a 2018 NARSAD Young Investigator grant (27023) from the Brain & Behavior Research Foundation.; Yoshiyuki Hirano was supported by AMED under Grant Number JP18dm0307002, JSPS KAKENHI Grant Number 16K04344; Marcelo Q. Hoexter was supported by Fundação de Amparo à Pesquisa do Estado de São Paulo (FAPESP, São Paulo Research Foundation; Grant no. 2011/21357-9); Fern Jaspers-Fayer was supported by Michael Smith Foundation for Health Research; Norbert Kathmann was supported by BMBF-01GW0724 from the Federal Ministry of Education and Research of Germany; Kathrin Koch was supported by Deutsche Forschungsgemeinschaft (DFG) grant (KO 3744/7-1); Gerd Kvale was supported by Funding by Helse Vest Health Authority (911754, 911880); Norwegian Research Council, HELSEFORSK 243675; Luisa Lazaro was supported by The Marató TV3 Foundation grants 01/2010 and 091710; The Carlos III Health Institute (PI040829) co-funded by FEDER funds/European Regional Development Fund (ERDF), a way to build Europe; AGAUR (2017 SGR 881); Ricardo Magalhães was supported by the FCT fellowship grant with the number PDE/BDE/113604/2015 from the PhD-iHES program; Rachel Marsh was supported by NIMH R21MH101441; Ignacio Martínez-Zalacaín was supported by Grant FI17/00294 from the Carlos III Health Institute. ; José M. Menchón was supported by Project grant PI16/00950 from the Carlos III Health Institute and AGAUR 2017 SGR 1247 from the Generalitat de Catalunya. ; Euripedes C. Miguel was supported by the Fundação de Amparo à Pesquisa do Estado de São Paulo (FAPESP, São Paulo Research Foundation; Grant no. 2011/21357-9); Pedro S Moreira was supported by the FCT fellowship grant with the number PDE/BDE/113601/2015 from the PhD-iHES program; Takashi Nakamae was supported by JSPS KAKENHI Grant Numbeer 16K19778 and 18K07608; Tomohiro Nakao was supported by Grant-in-Aid for Scientific Research (C) (22591262) (25461732) (16K10253) from the Japanese Ministry of Education, Culture, Sports, Science and Technology; Janardhanan. C. Narayanaswamy was supported by Government of India grants to Dr. Narayanaswamy from Department of Science and Technology (DST INSPIRE faculty grant -IFA12-LSBM-26) & Department of Biotechnology (BT/06/IYBA/2012); Joseph O'Neill was supported by NIMH grants R01MH081864 (to Drs. O'Neill and Piacentini) and R01MH085900 (to Drs. O'Neill and Feusner); John Piacentini was supported by NIMH grants R01MH081864 (to Drs. O'Neill and Piacentini) and R01MH085900 (to Drs. O'Neill and Feusner); Y.C. Janardhan Reddy was supported by Government of India grants to Prof. Reddy from Department of Science and Technology (SR/S0/HS/0016/2011) & Department of Biotechnology(No.BT/PR13334/Med/30/259/2009); H. Blair Simpson was supported by NIMH R21MH093889 and by the New York State Office of Mental Health; Carles Soriano-Mas was supported by Grant CPII16/00048 and Project grants PI13/01958 and PI16/00889 from the Carlos III Health Institute, co-funded by FEDER funds/European Regional Development Fund (ERDF), a way to build Europe. ; Gianfranco Spalletta was supported by Italian Ministry of Health RC13-14-15-16A; Emily R. Stern was supported by UL1TR000067/KL2TR00069 from the National Center for Advancing Translational Sciences. ; S. Evelyn Stewart was supported by Canadian Institutes of Health Research, Michael Smith Foundation for Health Research, British Columbia Provincial Health Services Authority; Guido A. van Wingen was supported by Netherlands Organization for Scientific Research (NWO/ZonMW Vidi 917.15.318); Ganesan Venkatasubramanian was supported by Wellcome-DBT India Alliance grant to Dr. Venkatasubramanian (500236/Z/11/Z); Zhen Wang was supported by National Natural Science Foundation of China (81371340) and the Shanghai Key Laboratory of Psychotic Disorders (No.13dz2260500). Akiko Nakagawa was JSPS KAKENHI Grant Number 26461762.

Disclosures

Justin T. Baker: Dr. Baker has received consulting income from Pear Therapeutics and Niraax Therapeutics; Brian P. Brennan: Dr. Brennan has received consulting fees from Rugen Therapeutics and Nobilis Therapeutics and research grant support from Eli Lilly, Transcept Pharmaceuticals, and Biohaven Pharmaceuticals.; David Mataix-Cols: Prof. Mataix-Cols receives royalties for contributing articles to UpToDate, Wolters Kluwer Health, and fees from Elsevier in his role as associate editor; H. Blair Simpson: Dr. Simpson has received royalties from UpToDate, Inc and Cambridge University Press and is currently receiving research support from Biohaven for a multi-site industry-sponsored clinical trial.

All other authors report no biomedical financial interests or potential conflicts of interest.

References

1. Ruscio AM, Stein DJ, Chiu WT, Kessler RC (2010): The epidemiology of obsessive-compulsive disorder in the National Comorbidity Survey Replication. *Mol Psychiatry*. 15:53-63.
2. Wittchen HU, Jacobi F (2005): Size and burden of mental disorders in Europe--a critical review and appraisal of 27 studies. *Eur Neuropsychopharmacol*. 15:357-376.
3. Nestadt G, Samuels J, Riddle M, Bienvenu OJ, 3rd, Liang KY, LaBuda M, et al. (2000): A family study of obsessive-compulsive disorder. *Arch Gen Psychiatry*. 57:358-363.
4. Pauls DL, Abramovitch A, Rauch SL, Geller DA (2014): Obsessive-compulsive disorder: an integrative genetic and neurobiological perspective. *Nat Rev Neurosci*. 15:410-424.
5. Geschwind DH, Flint J (2015): Genetics and genomics of psychiatric disease. *Science*. 349:1489-1494.
6. Hugdahl K, Davidson RJ (2004): *The asymmetrical brain*. MIT press.
7. Zago L, Petit L, Jobard G, Hay J, Mazoyer B, Tzourio-Mazoyer N, et al. (2017): Pseudoneglect in line bisection judgement is associated with a modulation of right hemispheric spatial attention dominance in right-handers. *Neuropsychologia*. 94:75-83.
8. Zhen Z, Kong XZ, Huang L, Yang Z, Wang X, Hao X, et al. (2017): Quantifying the variability of scene-selective regions: Interindividual, interhemispheric, and sex differences. *Hum Brain Mapp*. 38:2260-2275.
9. Coan JA, Allen JJB (2004): Frontal EEG asymmetry as a moderator and mediator of emotion. *Biological Psychology*. 67:7-49.
10. Wheeler RE, Davidson RJ, Tomarken AJ (1993): Frontal Brain Asymmetry and Emotional Reactivity - a Biological Substrate of Affective Style. *Psychophysiology*. 30:82-89.
11. Vigneau M, Beaucousin V, Herve PY, Duffau H, Crivello F, Houde O, et al. (2006): Meta-analyzing left hemisphere language areas: Phonology, semantics, and sentence processing. *Neuroimage*. 30:1414-1432.
12. Corballis MC (2003): From mouth to hand: gesture, speech, and the evolution of right-handedness. *Behav Brain Sci*. 26:199-208; discussion 208-160.
13. Crow TJ (1990): Temporal-Lobe Asymmetries as the Key to the Etiology of Schizophrenia. *Schizophrenia Bulletin*. 16:433-&.
14. Yucel M, Stuart GW, Maruff P, Wood SJ, Savage GR, Smith DJ, et al. (2002): Paracingulate morphologic differences in males with established schizophrenia: a magnetic resonance imaging morphometric study. *Biol Psychiatry*. 52:15-23.
15. Eyler LT, Pierce K, Courchesne E (2012): A failure of left temporal cortex to specialize for language is an early emerging and fundamental property of autism. *Brain*. 135:949-960.
16. Altarelli I, Leroy F, Monzalvo K, Fluss J, Billard C, Dehaene-Lambertz G, et al. (2014): Planum temporale asymmetry in developmental dyslexia: Revisiting an old question. *Hum Brain Mapp*. 35:5717-5735.
17. Kuelz AK, Hohagen F, Voderholzer U (2004): Neuropsychological performance in obsessive-compulsive disorder: a critical review. *Biol Psychol*. 65:185-236.
18. Abramovitch A, Abramowitz JS, Mittelman A (2013): The neuropsychology of adult obsessive-compulsive disorder: a meta-analysis. *Clinical psychology review*. 33:1163-1171.
19. Kuskowski MA, Malone SM, Kim SW, Dysken MW, Okaya AJ, Christensen KJ (1993): Quantitative EEG in obsessive-compulsive disorder. *Biol Psychiatry*. 33:423-430.
20. Maril S, Hermesh H, Gross-Isseroff R, Tomer R (2007): Spatial attention and neural asymmetry in obsessive-compulsive disorder. *Psychiatry Res*. 153:189-193.
21. Rao NP, Arasappa R, Reddy NN, Venkatasubramanian G, Reddy Y.C. J (2015): Lateralisation abnormalities in obsessive-compulsive disorder: a line bisection study. *Acta Neuropsychiatrica*. 27:242-247.
22. Ischebeck M, Endrass T, Simon D, Kathmann N (2014): Altered frontal EEG asymmetry in obsessive-compulsive disorder. *Psychophysiology*. 51:596-601.

23. Wexler BE, Goodman WK (1991): Cerebral laterality, perception of emotion, and treatment response in obsessive-compulsive disorder. *Biol Psychiatry*. 29:900-908.
24. Schienle A, Schafer A, Stark R, Walter B, Vaitl D (2005): Neural responses of OCD patients towards disorder-relevant, generally disgust-inducing and fear-inducing pictures. *Int J Psychophysiol*. 57:69-77.
25. Simon D, Kaufmann C, Musch K, Kischkel E, Kathmann N (2010): Fronto-striato-limbic hyperactivation in obsessive-compulsive disorder during individually tailored symptom provocation. *Psychophysiology*. 47:728-738.
26. Rao NP, Reddy YC, Kumar KJ, Kandavel T, Chandrashekar CR (2008): Are neuropsychological deficits trait markers in OCD? *Prog Neuropsychopharmacol Biol Psychiatry*. 32:1574-1579.
27. Shagass C, Roemer RA, Straumanis JJ, Josiassen RC (1984): Distinctive Somatosensory Evoked-Potential Features in Obsessive-Compulsive Disorder. *Biological Psychiatry*. 19:1507-1524.
28. Tot S, Ozge A, Comelekoglu U, Yazici K, Bal N (2002): Association of QEEG findings with clinical characteristics of OCD: evidence of left frontotemporal dysfunction. *Can J Psychiatry*. 47:538-545.
29. Shin YW, Ha TH, Kim SY, Kwon JS (2004): Association between EEG alpha power and visuospatial function in obsessive-compulsive disorder. *Psychiatry Clin Neurosci*. 58:16-20.
30. Towey J, Bruder G, Tenke C, Leite P, Decaria C, Friedman D, et al. (1993): Event-Related Potential and Clinical Correlates of Neurodysfunction in Obsessive-Compulsive Disorder. *Psychiatry Research*. 49:167-181.
31. Rus OG, Reess TJ, Wagner G, Zimmer C, Zaudig M, Koch K (2017): Functional and structural connectivity of the amygdala in obsessive-compulsive disorder. *Neuroimage Clin*. 13:246-255.
32. Ahmari SE, Spellman T, Douglass NL, Kheirbek MA, Simpson HB, Deisseroth K, et al. (2013): Repeated cortico-striatal stimulation generates persistent OCD-like behavior. *Science*. 340:1234-1239.
33. Mondino M, Haesebaert F, Poulet E, Saoud M, Brunelin J (2015): Efficacy of Cathodal Transcranial Direct Current Stimulation Over the Left Orbitofrontal Cortex in a Patient With Treatment-Resistant Obsessive-Compulsive Disorder. *J ECT*. 31:271-272.
34. Peng Z, Li G, Shi F, Shi C, Yang Q, Chan RC, et al. (2015): Cortical asymmetries in unaffected siblings of patients with obsessive-compulsive disorder. *Psychiatry Res*. 234:346-351.
35. Garber HJ, Ananth JV, Chiu LC, Griswold VJ, Oldendorf WH (1989): Nuclear magnetic resonance study of obsessive-compulsive disorder. *Am J Psychiatry*. 146:1001-1005.
36. Button KS, Ioannidis JPA, Mokrysz C, Nosek BA, Flint J, Robinson ESJ, et al. (2013): Power failure: why small sample size undermines the reliability of neuroscience. *Nature Reviews Neuroscience*. 14:365-376.
37. Thompson PM, Stein JL, Medland SE, Hibar DP, Vasquez AA, Renteria ME, et al. (2014): The ENIGMA Consortium: large-scale collaborative analyses of neuroimaging and genetic data. *Brain imaging and behavior*. 8:153-182.
38. Boedhoe P, Schmaal L, Abe Y, Alonso P, Ameis SH, Anticevic A, et al. (2018): Cortical Abnormalities Associated With Pediatric and Adult Obsessive-Compulsive Disorder: Findings From the ENIGMA Obsessive-Compulsive Disorder Working Group. *Am J Psychiatry*. 175:453-462.
39. Boedhoe P, Schmaal L, Abe Y, Ameis SH, Arnold PD, Batistuzzo MC, et al. (2017): Distinct Subcortical Volume Alterations in Pediatric and Adult OCD: A Worldwide Meta- and Mega-Analysis. *Am J Psychiatry*. 174:60-69.
40. Kong X-Z, Mathias SR, Guadalupe T, Group ELW, Glahn DC, Franke B, et al. (2018): Mapping cortical brain asymmetry in 17,141 healthy individuals worldwide via the ENIGMA Consortium. *PNAS*.
41. Kurth F, Gaser C, Luders E (2015): A 12-step user guide for analyzing voxel-wise gray matter asymmetries in statistical parametric mapping (SPM). *Nature Protocols*. 10:293-304.
42. Leroy F, Cai Q, Bogart SL, Dubois J, Coulon O, Monzalvo K, et al. (2015): New human-specific brain landmark: the depth asymmetry of superior temporal sulcus. *Proc Natl Acad Sci U S A*. 112:1208-1213.

43. Guadalupe T, Mathias SR, vanErp TG, Whelan CD, Zwiers MP, Abe Y, et al. (2016): Human subcortical brain asymmetries in 15,847 people worldwide reveal effects of age and sex. *Brain Imaging Behav*.
44. van den Heuvel OA, van Wingen G, Soriano-Mas C, Alonso P, Chamberlain SR, Nakamae T, et al. (2016): Brain circuitry of compulsivity. *Eur Neuropsychopharmacol*. 26:810-827.
45. Desikan RS, Segonne F, Fischl B, Quinn BT, Dickerson BC, Blacker D, et al. (2006): An automated labeling system for subdividing the human cerebral cortex on MRI scans into gyral based regions of interest. *Neuroimage*. 31:968-980.
46. Zhong S, He Y, Shu H, Gong G (2017): Developmental Changes in Topological Asymmetry Between Hemispheric Brain White Matter Networks from Adolescence to Young Adulthood. *Cereb Cortex*. 27:2560-2570.
47. Schmaal L, Hibar DP, Samann PG, Hall GB, Baune BT, Jahanshad N, et al. (2017): Cortical abnormalities in adults and adolescents with major depression based on brain scans from 20 cohorts worldwide in the ENIGMA Major Depressive Disorder Working Group. *Mol Psychiatry*. 22:900-909.
48. Schmaal L, Veltman DJ, van Erp TG, Samann PG, Frodl T, Jahanshad N, et al. (2016): Subcortical brain alterations in major depressive disorder: findings from the ENIGMA Major Depressive Disorder working group. *Mol Psychiatry*. 21:806-812.
49. van Erp TGM, Walton E, Hibar DP, Schmaal L, Jiang W, Glahn DC, et al. (2018): Cortical Brain Abnormalities in 4474 Individuals With Schizophrenia and 5098 Control Subjects via the Enhancing Neuro Imaging Genetics Through Meta Analysis (ENIGMA) Consortium. *Biol Psychiatry*.
50. Logue MW, van Rooij SJH, Dennis EL, Davis SL, Hayes JP, Stevens JS, et al. (2018): Smaller Hippocampal Volume in Posttraumatic Stress Disorder: A Multisite ENIGMA-PGC Study: Subcortical Volumetry Results From Posttraumatic Stress Disorder Consortia. *Biol Psychiatry*. 83:244-253.
51. van Rooij D, Anagnostou E, Arango C, Auzias G, Behrmann M, Busatto GF, et al. (2018): Cortical and Subcortical Brain Morphometry Differences Between Patients With Autism Spectrum Disorder and Healthy Individuals Across the Lifespan: Results From the ENIGMA ASD Working Group. *Am J Psychiatry*. 175:359-369.
52. Ojemann GA (1977): Asymmetric function of the thalamus in man. *Ann N Y Acad Sci*. 299:380-396.
53. Behrens TEJ, Johansen-Berg H, Woolrich MW, Smith SM, Wheeler-Kingshott CAM, Boulby PA, et al. (2003): Non-invasive mapping of connections between human thalamus and cortex using diffusion imaging. *Nature Neuroscience*. 6:750-757.
54. Mataix-Cols D, Frost RO, Pertusa A, Clark LA, Saxena S, Leckman JF, et al. (2010): Hoarding disorder: a new diagnosis for DSM-V? *Depress Anxiety*. 27:556-572.
55. Smith KS, Tindell AJ, Aldridge JW, Berridge KC (2009): Ventral pallidum roles in reward and motivation. *Behav Brain Res*. 196:155-167.
56. Mataix-Cols D, Boman M, Monzani B, Ruck C, Serlachius E, Langstrom N, et al. (2013): Population-based, multigenerational family clustering study of obsessive-compulsive disorder. *JAMA psychiatry*. 70:709-717.
57. Hibar DP, Cheung JW, Medland SE, Mufford MS, Jahanshad N, Dalvie S, et al. (2018): Significant concordance of genetic variation that increases both the risk for obsessive-compulsive disorder and the volumes of the nucleus accumbens and putamen. *Br J Psychiatry*. 213:430-436.
58. International Obsessive Compulsive Disorder Foundation Genetics C, Studies OCDCGA (2018): Revealing the complex genetic architecture of obsessive-compulsive disorder using meta-analysis. *Mol Psychiatry*. 23:1181-1188.
59. Johansen-Berg H, Behrens TEJ, Sillery E, Ciccarelli O, Thompson AJ, Smith SM, et al. (2005): Functional-anatomical validation and individual variation of diffusion tractography-based segmentation of the human thalamus. *Cerebral Cortex*. 15:31-39.
60. Maingault S, Tzourio-Mazoyer N, Mazoyer B, Crivello F (2016): Regional correlations between cortical thickness and surface area asymmetries: A surface-based morphometry study of 250 adults. *Neuropsychologia*. 93:350-364.

61. Van Essen DC, Glasser MF, Dierker DL, Harwell J, Coalson T (2012): Parcellations and hemispheric asymmetries of human cerebral cortex analyzed on surface-based atlases. *Cereb Cortex*. 22:2241-2262.

Table 1. Summary information on the case-control datasets included in the present study.

Group	Site	Field Strength	Age in Years		Male (%)		N Controls	N OCD	Total N
			Controls	OCD	Controls	OCD			
Pediatric	James	1.5 T	16.63 (1.23)	16.3 (1.42)	58	54	12	13	25
	Lazaro	1.5 T	14.63 (2.3)	14.61 (2.04)	47	58	32	31	63
	Buitelaar	1.5 T	10.93 (1.04)	10.57 (1.41)	72	64	61	22	83
	Fitzgerald	3 T	12.96 (2.73)	14.17 (2.59)	51	48	59	62	121
	Gruner	3 T	14.19 (2.21)	14.33 (2.09)	52	57	23	23	46
	Arnold	3 T	12.3 (2.19)	12.86 (2.35)	54	61	13	36	49
	Hoexter	3 T	12 (2.42)	12.61 (2.45)	57	61	28	28	56
	Huyser	3 T	13.32 (2.55)	13.59 (2.47)	36	37	25	27	52
	Stewart	3 T	14.02 (3.48)	15.04 (2.68)	40	39	30	28	58
	Lazaro	3 T	14.57 (2.1)	14.57 (2.04)	55	60	44	58	102
	Nurmi	3 T	13.3 (2.49)	12.53 (2.84)	50	54	36	59	95
	Walitza	3 T	14.64 (1.34)	15.68 (1.45)	50	81	20	16	36
	Reddy	3 T	13.07 (2.06)	14.56 (1.98)	50	56	14	18	32
	Marsh	3 T	9.14 (2.48)	12.12 (3.4)	57	52	14	25	39
	Hirano	3 T	15.33 (1.03)	14 (2.18)	67	65	6	20	26
	Soreni	3 T	11.09 (3.02)	13.09 (2.47)	50	37	22	35	57
Pediatric Samples Combined			13.06 (2.77)	13.67 (2.65)	53	54	439	501	940
Adult	Menchon	1.5 T	33.06 (10.19)	34.83 (9.17)	45	50	66	117	183
	Cheng	1.5 T	31.43 (7.96)	30.63 (10.21)	33	38	40	24	64
	KwonNMC	1.5 T	24.05 (3.63)	24.76 (5.36)	56	76	104	45	149
	KwonSNU	1.5 T	24.89 (5.35)	28.1 (6.71)	64	63	45	41	86
	Nakamae	1.5 T	30.44 (7.9)	31.61 (9.15)	46	48	48	82	130
	Morgado	1.5 T	27.58 (6.23)	27.69 (7.4)	38	47	53	59	112
	Mataix_Cols	1.5 T	36.12 (11.26)	38.68 (10.9)	36	43	33	44	77
	Reddy	1.5 T	27.22 (6.45)	27.45 (6.31)	74	59	46	44	90
	Hoexter	1.5 T	27.62 (7.75)	31.46 (10.06)	35	44	37	50	87
	van den Heuvel	1.5 T	31.57 (7.67)	33.54 (9.19)	39	30	49	54	103
	Beucke	1.5 T	31.92 (9.5)	32.41 (9.74)	49	50	104	92	196
	Cheng	3 T	26.19 (4.18)	32.89 (10.57)	28	55	95	56	151
	Nakamae	3 T	29.57 (7.27)	32.82 (9.74)	45	35	42	34	76
	Brennan	3 T	32.38 (12.14)	28.84 (9.99)	45	56	29	98	127
	van den Heuvel	3 T	39.61 (11.37)	38.32 (10.07)	47	48	38	42	80
	Denys	3 T	39.64 (10.32)	35.26 (9.17)	44	26	25	31	56
	Kwon	3 T	26.26 (6.9)	26.7 (7.28)	61	62	89	90	179
	Benedetti	3 T	33.98	35.02	73	71	62	66	128

			(12.35)	(10.39)					
	Hirano	3 T	30.95 (8.36)	33.11 (7.82)	45	36	44	47	91
	Koch	3 T	30.27 (9.04)	30.91 (9.55)	39	37	74	76	150
	Stein	3 T	30.59 (10.76)	30.48 (10.63)	38	48	29	23	52
	Tolin	3 T	48 (11.87)	32.11 (12.04)	22	67	32	27	59
	Simpson	3 T	28.27 (8.04)	29.62 (7.98)	52	52	33	33	66
	Nakao	3 T	39.34 (12.99)	36.6 (10.02)	39	42	41	81	122
	Spalletta	3 T	36.52 (10.55)	36.67 (11.56)	59	67	128	84	212
	Stern	3 T	28.17 (7.15)	27.87 (6.9)	44	33	18	15	33
	Wang	3 T	26.24 (7.55)	29.47 (9.33)	54	55	37	53	90
	Nurmi	3 T	30.76 (11.77)	33.31 (11.04)	56	51	25	49	74
	Walitza	3 T	32.89 (9.21)	30.72 (7.76)	28	47	18	17	35
	Reddy	3 T	26.59 (4.88)	29.5 (6.74)	64	53	170	203	373
Adult Samples Combined			30.55 (9.73)	31.74 (9.66)	50	51	1654	1777	3431

Site indicate the representative author of each dataset; Numbers in parenthesis indicate the standard deviation of age.

Figure 1. Effect size (Cohen's *d*) distributions for diagnosis on regional AIs in the pediatric (left) and adult (right) data.

Figure 2. Subcortical structures showing altered volumetric asymmetry in pediatric OCD patients: the thalamus and the pallidum. The violin plots show the distributions and group differences of the volume asymmetry (A) and the lateral volume measures (in mm^3) in each hemisphere (B) for the thalamus and the pallidum. Note that the main analyses were based on linear mixed-effect modelling with 'dataset' as a random-effect term, whereas data are plotted here without correction for the 'dataset' variable, for display purposes only.

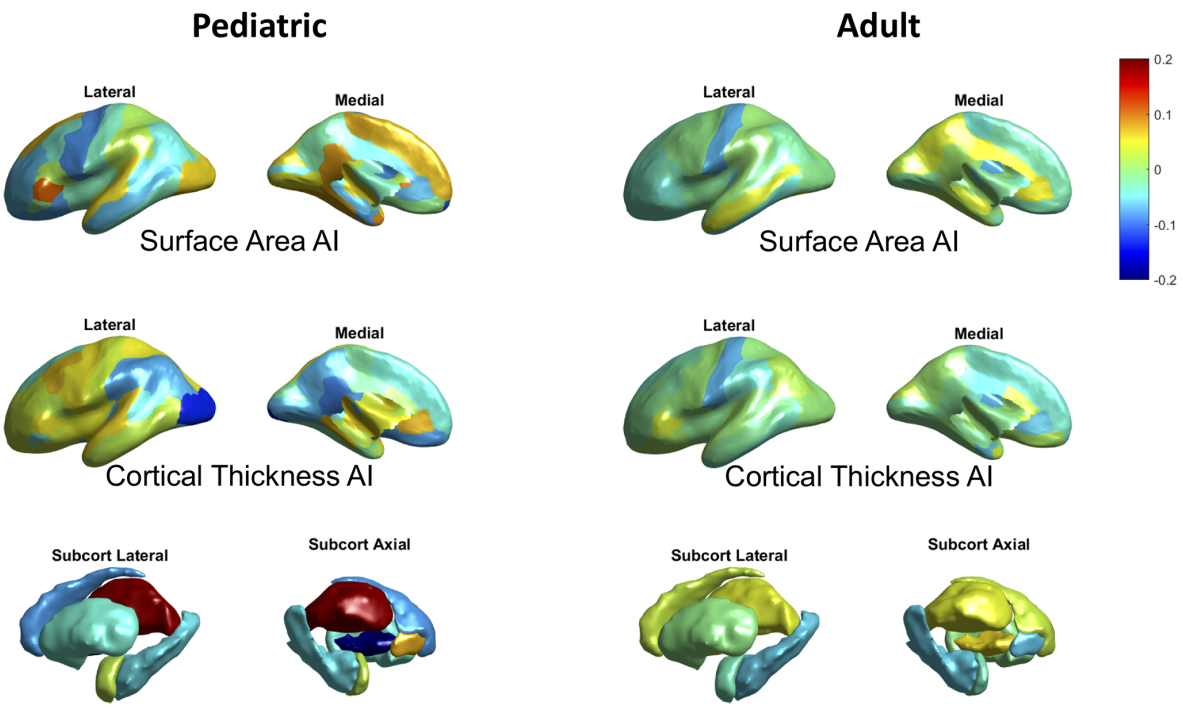

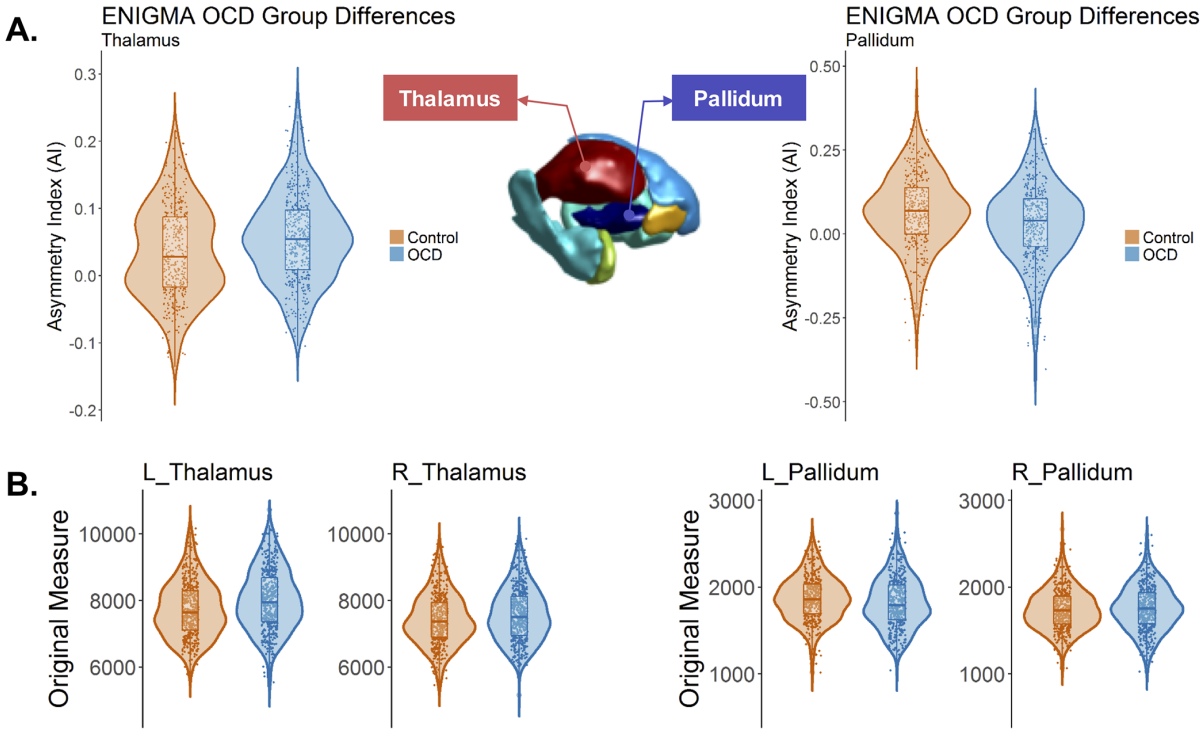

Mapping Cortical and Subcortical Asymmetry in Obsessive-Compulsive Disorder: Findings From the ENIGMA Consortium

Supplement 1

Supplemental Methods and Materials

Datasets. The datasets used in this study were provided by members of the OCD Working Group within the ENIGMA Consortium (1). There were 46 independent datasets from 16 countries (Brazil, Canada, China, Germany, India, Italy, Japan, the Netherlands, Portugal, Republic of Korea, Sweden, South-Africa, Spain, Switzerland, United Kingdom, and United States of America). Data comprised both subcortical and cortical measures from a total of 2278 patients with OCD and 2093 healthy control subjects (16 pediatric datasets comprising 501 OCD patients and 439 healthy controls, and 30 adult datasets comprising 1777 OCD patients and 1654 healthy controls). Thirty-five and thirty-eight of these datasets were identical to those included in the previous ENIGMA subcortical (2) and cortical (3) studies respectively. Handedness information was not extensive within these datasets, but previous large-scale analyses in datasets of over 15,000 healthy subjects have indicated that handedness is of little relevance to the structural brain asymmetry measures analyzed here (4, 5). Basic demographic and clinical information are summarized in Table 1 and Figure S1-2; more details of the contributing datasets can be found in Table S1. All local institutional reviews boards permitted the use of extracted measures from their anonymized data. In addition, we leveraged publicly available summary statistics which describe the average form of brain regional asymmetries, based on our previous larger studies of healthy individuals (http://conxz.github.io/neurohemi; (4, 5)).

Image Acquisition and Processing. Structural T1-weighted MRI scans were acquired and processed locally at each collection site. Images were acquired at different field strengths (1.5 T and 3T). All images were analyzed using one automated and validated pipeline, i.e. “recon-all” as implemented in *FreeSurfer* (version 5.3). Briefly, the main stages of the processing pipeline include normalization of brain signal intensity, skull-stripping, white matter and gray matter segmentation, and delineation of the

gray-white interface (inner surface) and the pial surface (outer surface). Next, the surface is divided into separate cortical regions using an automated labeling approach, where not only location information based on a probabilistic surface-based atlas, but also local curvature and contextual information (e.g., sulcal and gyral geometry) of subject-specific surface are taken into consideration. Finally, for each subject, surface area and mean thickness was extracted for each of the 68 cortical regions (34 per hemisphere) in the Desikan-Killiany parcellation scheme (6), as well as total hemispheric surface area, and the average mean thickness over each hemisphere. We chose this parcellation scheme because it is well-established in the surface space, has been widely used in brain structure studies including previous ENIGMA consortium studies, and is feasible for large collaborative projects (see e.g. (5)). For more details on the image processing and data collection, please refer to (2, 3, 6). In addition, volumes of eight subcortical regions of interest, including seven subcortical structures (nucleus accumbens, amygdala, caudate, hippocampus, pallidum, putamen, and thalamus), and the lateral ventricle volume, were calculated. This segmentation is also part of the pipeline 'recon-all', and based on an atlas containing probabilistic information on the location of structures (7). All calculations were made in each subject's native space. Further processing and quality control for all datasets was then performed following standardized ENIGMA protocols (http://enigma.ini.usc.edu/protocols/imaging-protocols/), which include, briefly, extracting cortical and subcortical measures from *FreeSurfer* outputs, outlier detection, and visual quality checking. Finally, each dataset was prepared based on a unified table format, and shared with the central analysis team for this study.

Asymmetry Indexes. The main aim of this study was to investigate differences in subcortical and cortical asymmetry related to OCD. To this end, for each participant, and each subcortical or cortical measure, an Asymmetry Index (AI) was defined as *(L-R)/((L+R)/2)*, where L and R represent the corresponding left and right volume measures (from subcortical regions), or thickness and surface area measures (from cortical regions). Thus, positive and negative AI values indicate leftward and rightward asymmetry, respectively, for a given left-right paired measure. This AI formula has been widely used in previous brain asymmetry studies (8-10), including our own (4, 5, 11). In addition, it is important to note that in the definition of the AI, the difference (i.e., L-R) was normalized by use of the bilateral

measures as denominator (i.e., L+R), such that the measure does not scale with the overall magnitude of L and R. For this reason, we also did not adjust for intracranial volume (ICV) in our analyses. We previously showed that there are subtle associations between ICV and regional brain asymmetries in the general population (5). However, here we wished to capture the full extent of any OCD-asymmetry associations, regardless of whether underlying causal influences might also affect ICV. Therefore, we did not adjust for ICV in our main analysis. Nonetheless, we also repeated our analyses including ICV as a covariate effect, to confirm that results did not depend on this choice (Results are shown below).

In our main analyses, we did not exclude any data points in addition to those already excluded by the quality control procedures included in the ENIGMA protocols (see (2, 3) for further details on quality checking). However, we also repeated our analyses after excluding possible outliers on each AI, within each dataset and each diagnosis group, with a threshold of 2.5SD from the mean, in order to confirm that findings from the main analysis were not driven by extreme data points.

Case-control Analyses. Separately for the pediatric and adult data, and for each subcortical or cortical AI, we pooled data from all available individuals from each dataset, and used a mega-analytical framework to investigate the case-control effects. Specifically, for each AI, we used a linear mixed-effect model (using *lme4* R package, version 1.1-12), with AI as the outcome variable, and a binary indicator of diagnosis (0=healthy controls, 1=OCD patients) as the predictor of interest. In each model, a binary variable for sex, and a continuous measure for age (in years at time of scan) were included as confounding factors, and the categorical variable ‘dataset’ as a random-effect term. Model fit was checked visually by inspection of the plot of residuals versus fitted values, and the histogram and quantile-quantile (Q-Q) plots for the residual values. Condition number (i.e., Kappa) and variance inflation factor (VIF) were calculated in order to assess collinearity (troubling collinearity is indicated by Kappa values of 30, and/or VIF values of 5 or above). Coefficients of “Estimate”, “Std. Error”, and “t value” for the predictor of interest (i.e., diagnosis) were extracted from the model outputs, while significance (i.e., *p* value) was assessed using likelihood ratio tests to compare models with and without the predictor (using function *anova* from *stats* R package, version 3.2.5). Separately within each age

group (pediatric or adult), and separately for each type of asymmetry measure, i.e. 8 tests for subcortical volume AIs, 35 tests for cortical thickness AIs, 35 tests for cortical surface area AIs, the false-discovery-rate (FDR) correction procedure ($q <= 0.05$) was used to correct for multiple comparisons. Cohen's *d*, as effect size, was calculated for each effect based on its *t* value and the sample sizes (i.e., *N1* and *N2*) of each group, with the formula *t*sqrt(1/N1+1/N2)* (12). To investigate whether the effect sizes of diagnosis on cortical AIs were related between the pediatric and adult data, we calculated the correlations between the Cohen's d across all 34 cortical regions, separately for cortical thickness and surface area AIs.

We repeated the main analysis by additionally including age^2 as a confounding factor, in case of substantial non-linear effects on AIs (but this had very little effect, see Results). We also repeated the main analyses with regard to potential influences of MRI scanner field strength. In this analysis, in addition to sex and age, an additional binary predictor variable of scanner field strength (1.5T scanners versus 3T scanners) was included. We were interested in whether 1) scanner effects on the AIs were significant, and 2) whether any significant effects of diagnosis on AIs remained after controlling for effects related to differences in scanner field strength.

Separately for thickness and surface area, we additionally calculated an overall 'typicality score' per subject, which indexed how much a given subject deviated from the population mean asymmetry profile, when considered simultaneously across all 34 cortical regions. The typicality score for a given subject was calculated as the Spearman correlation coefficient between that the subject's AIs and the population mean AIs, across all 34 regions. Population data were based on summary statistics from more than 17,000 subjects drawn from the general population or healthy control datasets, which were available online (http://conxz.github.io/neurohemi; (5)). A lower typicality score indicates more deviation from the mean asymmetry profile in the population. We compared the typicality scores between OCD patients and controls, using the same linear mixed-effect model as used in the main analyses (i.e. correcting for sex, age and dataset), except that the outcome variable was now the typicality score. The hypothesis was that the overall asymmetry profile in OCD, as considered across multiple regions, might deviate from

the typical pattern more than for the control subjects in this study. No multiple testing correction was performed, as this was intended as an exploratory analysis.

OCD Case-only Analyses of Clinical Characteristics. For AIs which were potentially associated with OCD in the main analysis (see Results), we further investigated, within cases only, whether the following predictors were associated with the AIs: medication status (medication-free OCD cases vs. medicated cases), age at disease onset (in years), disease duration (in years), current anxiety comorbidity (categorical yes/no) and current depression comorbidity (categorical yes/no). In addition, we also tested these AIs in relation to OCD severity measures, which were the total score based on the Yale-Brown Obsessive Compulsive Scale (Y-BOCS) or Children's Yale-Brown Obsessive Compulsive Scale (CY-BOCS), and the absence or presence of 5 previously identified symptom dimensions derived from the Y-BOCS (or CY-BOCS) symptom checklist: aggression/checking; cleaning/contamination; sexual/religion; hoarding; ordering/symmetry (13-15). For more details of this scheme, please refer to (2, 3). Data for these case-only variables were available for the majority of cases (see Supplementary Table S1 for the available sample sizes within each dataset). The same linear mixed-effect model was used as the main analysis, again with AI as the outcome variable, except that the predictor variable 'diagnosis' was now replaced by one of the within-case predictor variables per model (e.g. medicated/unmedicated as a binary variable, age of onset as a continuous variable etc.). All case-only analyses were performed separately for each age groups (pediatric and adult). These post-hoc analyses were intended as purely exploratory, and no correction for multiple testing was applied.

Supplemental Results

Main Results for Adult Data. Regionally, only the postcentral gyrus showed a nominally significant AI difference between patients and controls, which involved both its thickness AI ($t = -2.10$, $p = 0.036$, $d = -0.073$) and surface area AI ($t = -2.12$, $p = 0.034$, $d = -0.074$), but these effects could not survive correction for multiple testing. No other case-control comparisons of either subcortical or cortical AIs showed significant effects in the adult data (uncorrected ps >0.05).

When repeating the main analysis including age2 additionally in the model, all of the Cohen's d for the effects of diagnosis remained within 0.005 of their values before having included age2, and the same AI (adult global surface area) remained significant after FDR correction. None of the AIs showed significant scanner effects in the adult data (ps >0.05), and the effect of diagnosis on the global surface area AI remained when adding scanner field strength as a predictor variable to the model (diagnosis t = -2.44, p = 0.015, d = -0.085).

Additional Analyses. Our previous large-scale study has shown significant relationships between ICV and brain asymmetries, although the effect sizes are subtle (5). We repeated our analyses after additionally adjusting for ICV. Results showed that the main results remained: pediatric thalamus volume asymmetry: t = 2.85, p = 0.0045, d = 0.19; pediatric pallidum volume asymmetry: t = -3.07, p = 0.0022, d = -0.20; adult global hemispheric surface area asymmetry: t = -2.43, p = 0.015, d = -0.85). These findings suggest that adjusting for ICV had little impact on OCD case-control differences in brain asymmetries.

Regarding the adult OCD patients, the previous study showed a larger pallidum (again left plus right) than controls, driven by patients with a childhood-onset of disease (2). But we saw no significant effects on the asymmetry of this structure in the adult patients. We repeated our analyses with data for each subgroup of age of onset of disease: early-onset (i.e., before 18 years old) and late-onset patients (i.e., after 18 years old). No significant differences were found in either subgroup. Specifically, in the early-onset subgroup, neither asymmetry of the thalamus or pallidum showed significant differences (thalamus: t = 1.37, p = 0.17; pallidum: t = -0.028, p = 0.98). Similar null results were found in the late-onset subgroup (thalamus: t = 1.82, p = 0.07; pallidum: t = -0.48, p = 0.63). We further compared the effects between two subgroups, and found no significant differences (thalamus: t = 1.56, p = 0.12; pallidum: t = -0.088, p = 0.93).

Supplemental Tables

All supplemental tables (Tables S1-S7) are available in a separate Excel file.

Supplemental Figures

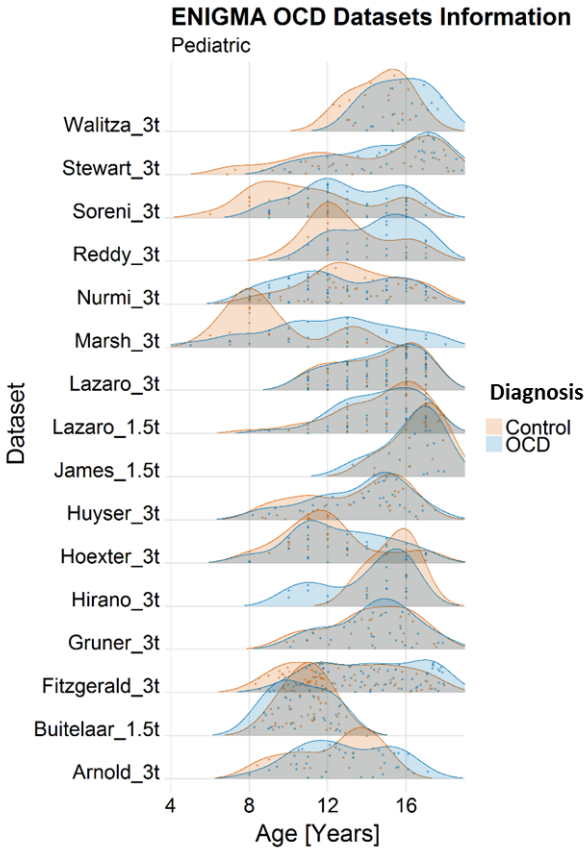

Figure S1. Age distributions of participants in each pediatric dataset.

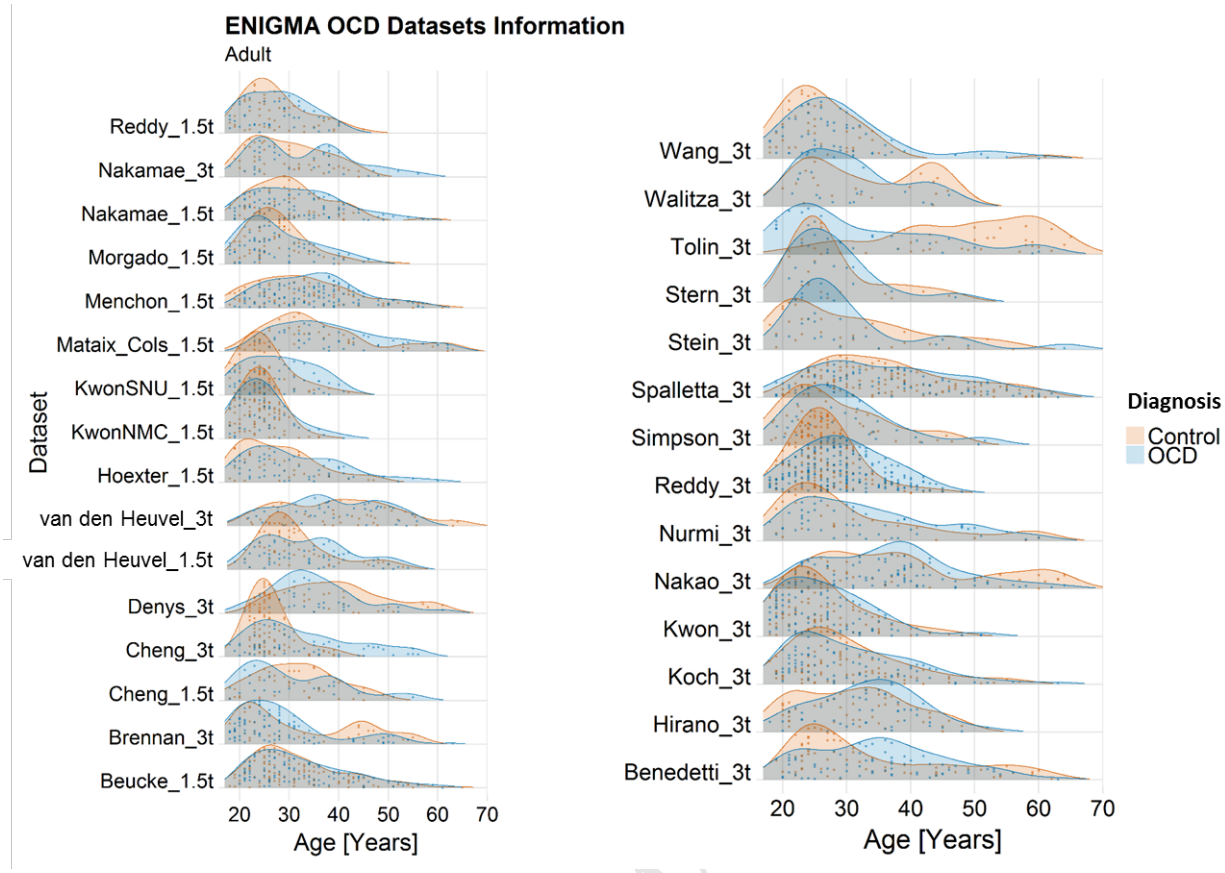

Figure S2. Age distributions of participants in each adult dataset.

Supplemental References

1. Thompson PM, Stein JL, Medland SE, Hibar DP, Vasquez AA, Renteria ME, et al. (2014): The ENIGMA Consortium: large-scale collaborative analyses of neuroimaging and genetic data. *Brain imaging and behavior*. 8:153-182.
2. Boedhoe P, Schmaal L, Abe Y, Ameis SH, Arnold PD, Batistuzzo MC, et al. (2017): Distinct Subcortical Volume Alterations in Pediatric and Adult OCD: A Worldwide Meta- and Mega-Analysis. *Am J Psychiatry*. 174:60-69.
3. Boedhoe P, Schmaal L, Abe Y, Alonso P, Ameis SH, Anticevic A, et al. (2018): Cortical Abnormalities Associated With Pediatric and Adult Obsessive-Compulsive Disorder: Findings From the ENIGMA Obsessive-Compulsive Disorder Working Group. *Am J Psychiatry*. 175:453-462.
4. Guadalupe T, Mathias SR, vanErp TG, Whelan CD, Zwiers MP, Abe Y, et al. (2016): Human subcortical brain asymmetries in 15,847 people worldwide reveal effects of age and sex. *Brain Imaging Behav*.
5. Kong X-Z, Mathias SR, Guadalupe T, Group ELW, Glahn DC, Franke B, et al. (2018): Mapping cortical brain asymmetry in 17,141 healthy individuals worldwide via the ENIGMA Consortium. *PNAS*.
6. Desikan RS, Segonne F, Fischl B, Quinn BT, Dickerson BC, Blacker D, et al. (2006): An automated labeling system for subdividing the human cerebral cortex on MRI scans into gyral based regions of interest. *Neuroimage*. 31:968-980.
7. Fischl B, Salat DH, Busa E, Albert M, Dieterich M, Haselgrove C, et al. (2002): Whole brain segmentation: Automated labeling of neuroanatomical structures in the human brain. *Neuron*. 33:341-355.
8. Kurth F, Gaser C, Luders E (2015): A 12-step user guide for analyzing voxel-wise gray matter asymmetries in statistical parametric mapping (SPM). *Nature Protocols*. 10:293-304.
9. Leroy F, Cai Q, Bogart SL, Dubois J, Coulon O, Monzalvo K, et al. (2015): New human-specific brain landmark: the depth asymmetry of superior temporal sulcus. *Proc Natl Acad Sci U S A*. 112:1208-1213.
10. Zhong S, He Y, Shu H, Gong G (2017): Developmental Changes in Topological Asymmetry Between Hemispheric Brain White Matter Networks from Adolescence to Young Adulthood. *Cereb Cortex*. 27:2560-2570.
11. Zhen Z, Kong XZ, Huang L, Yang Z, Wang X, Hao X, et al. (2017): Quantifying the variability of scene-selective regions: Interindividual, interhemispheric, and sex differences. *Hum Brain Mapp*. 38:2260-2275.
12. Nakagawa S, Cuthill IC (2007): Effect size, confidence interval and statistical significance: a practical guide for biologists. *Biological reviews of the Cambridge Philosophical Society*. 82:591-605.
13. Scahill L, Riddle MA, McSwiggin-Hardin M, Ort SI, King RA, Goodman WK, et al. (1997): Children's Yale-Brown Obsessive Compulsive Scale: reliability and validity. *J Am Acad Child Adolesc Psychiatry*. 36:844-852.
14. Goodman WK, Price LH, Rasmussen SA, Mazure C, Fleischmann RL, Hill CL, et al. (1989): The Yale-Brown Obsessive Compulsive Scale. I. Development, use, and reliability. *Arch Gen Psychiatry*. 46:1006-1011.
15. Mataix-Cols D, Fullana MA, Alonso P, Menchon JM, Vallejo J (2004): Convergent and discriminant validity of the Yale-Brown Obsessive-Compulsive Scale Symptom Checklist. *Psychother Psychosom*. 73:190-196.

Group	Site	Country	Field Stren	Age (years)	Age (years)	Male (%), H	Male (%), C	Heathy Cor	OCD Patier	Total (N)	Medicated	YBOCSMea	YBOCSSD	YBOCSN	AgeOnsetM	AgeOnsetS	AgeOnsetN	ComorbidA	AnxiN	ComorbidE	DeprN
2_pediatric	Pediatric C	James	UK	1.5	16.63 (1.23	16.3 (1.42)	58	54	12	13	25	13	13.84615	13	5.857277	11.45385	13	2.773871	0.384615	13	0.384615	13
2_pediatric	Lazaro	Spain	1.5	14.63 (2.3)	14.61 (2.04	47	58	32	31	63	31	22.22581	31	5.964951	12.41935	31	2.17216	0.16129	31	0.032258	31
2_pediatric	Buitelaar	Netherland	1.5	10.93 (1.04	10.57 (1.41	72	64	61	22	83	10	NA	0	NA	NA	0	NA	0	0	0	0
2_pediatric	Fitzgerald	USA	3	12.96 (2.73	14.17 (2.59	51	48	59	62	121	62	19.10484	62	8.190927	9.886177	62	3.145974	0.5	62	0.064516	62
2_pediatric	Gruner	USA	3	14.19 (2.21	14.33 (2.09	52	57	23	23	46	23	26.86957	23	4.475228	NA	0	NA	0.434783	23	0.391304	23
2_pediatric	Arnold	Canada	3	12.3 (2.19)	12.86 (2.35	54	61	13	36	49	34	20.92424	33	7.818369	8.666667	33	2.569857	0.277778	35	0.194444	34
2_pediatric	Hoexter	Brazil	3	12 (2.42)	12.61 (2.45	57	61	28	28	56	28	26.92857	28	5.429198	7.178571	28	3.019119	0.75	28	0.214286	28
2_pediatric	Huyser	Netherland	3	13.32 (2.55	13.59 (2.47	36	37	25	27	52	27	25.11111	27	5.048483	10.92481	27	2.808279	0.481481	27	0.259259	27
2_pediatric	Stewart	Canada	3	14.02 (3.48	15.04 (2.68	40	39	30	28	58	28	13.39286	27	6.712836	9.24	25	3.058867	0.357143	28	0.071429	28
2_pediatric	Lazaro	Spain	3	14.57 (2.1)	14.57 (2.04	55	60	44	58	102	58	18.58621	58	7.358095	12.01724	58	2.431456	0.275862	58	0.051724	58
2_pediatric	Nurmi	USA	3	13.3 (2.49)	12.53 (2.84	50	54	36	59	95	59	24.05085	59	3.980226	NA	0	NA	0.033898	57	0.016949	57
2_pediatric	Walitza	Switzerland	3	14.64 (1.34	15.68 (1.45	50	81	20	16	36	16	14.6875	14	10.39691	11.0625	16	2.205108	0.5	16	0.0625	16
2_pediatric	Reddy	India	3	13.07 (2.06	14.56 (1.98	50	56	14	18	32	18	22.55556	18	7.342241	13.11111	18	2.111283	0.222222	18	0.055556	18
2_pediatric	Marsh	USA	3	9.14 (2.48)	12.12 (3.4)	57	52	14	25	39	25	24.4	25	4.890467	9.32	25	3.448671	0.72	25	0	25
2_pediatric	Hirano	Japan	3	15.33 (1.03	14 (2.18)	67	65	6	20	26	20	26.89474	19	6.244062	11.9	20	2.35975	0.1	20	0	20
2_pediatric	Soreni	Canada	3	11.09 (3.02	13.09 (2.47	50	37	22	35	57	34	21.67647	33	5.563521	NA	0	NA	0.171429	8	0	28
1_adult	Adult Coho	Menchon		1.5	33.06 (10.1	34.83 (9.17	45	50	66	117	183	117	25.49573	117	5.839261	21.4359	117	8.476524	0.205128	117	0.188034	117
1_adult		Cheng	China	1.5	31.43 (7.96	30.63 (10.2	33	38	40	24	64	24	31	24	6.072031	26.83333	24	10.39509	0.5	24	0.166667	24
1_adult		KwonNMC	Republic of	1.5	24.05 (3.63	24.76 (5.36	56	76	104	45	149	45	20.22222	45	6.037342	17.44444	45	5.159085	0	45	0	45
1_adult		KwonSNU	Republic of	1.5	24.89 (5.35	28.1 (6.71)	64	63	45	41	86	41	23.47222	36	6.652545	18.12195	41	7.032763	0	41	0.02439	41
1_adult		Nakamae	Japan	1.5	30.44 (7.9)	31.61 (9.15	46	48	48	82	130	82	24.82927	82	6.537272	24.73171	82	8.836022	0.097561	82	0.231707	82
1_adult		Morgado	Portugal	1.5	27.58 (6.23	27.69 (7.4)	38	47	53	59	112	59	25.94643	56	5.788451	NA	0	NA	0	0	0	0
1_adult		Mataix_Co	Sweden	1.5	36.12 (11.2	38.68 (10.9	36	43	33	44	77	32	25.85714	21	7.702504	18.39394	33	9.175168	0.272727	24	0.340909	38
1_adult		Reddy	India	1.5	27.22 (6.45	27.45 (6.31	74	59	46	44	90	44	25.75	44	7.28849	21.65909	44	7.498661	0.159091	37	0.181818	43
1_adult		Hoexter	Brazil	1.5	27.62 (7.75	31.46 (10.0	35	44	37	50	87	50	27.2	50	6.094494	13.1	50	7.028368	0.62	50	0.54	50
1_adult		van den He	Netherland	1.5	31.57 (7.67	33.54 (9.19	39	30	49	54	103	54	22.70588	51	6.132843	14.41176	51	7.702406	0.203704	34	0.333333	38
1_adult		Beucke	Germany	1.5	31.92 (9.5)	32.41 (9.74	49	50	104	92	196	92	20.06977	86	7.064061	17.1791	67	7.808165	0.119565	92	0.184783	92
1_adult		Cheng	China	3	26.19 (4.18	32.89 (10.5	28	55	95	56	151	56	28.21429	56	6.320858	27.23214	56	10.70088	0.892857	56	0.285714	56
1_adult		Nakamae	Japan	3	29.57 (7.27	32.82 (9.74	45	35	42	34	76	34	22.05882	34	6.564095	25.05882	34	8.841847	0.088235	32	0.205882	32
1_adult		Brennan	USA	3	32.38 (12.1	28.84 (9.99	45	56	29	98	127	98	NA	0	NA	NA	0	NA	0	0	0	0
1_adult		van den He	Netherland	3	39.61 (11.3	38.32 (10.0	47	48	38	42	80	42	21.47619	42	6.141574	15.48718	39	6.866669	0.404762	42	0.52381	42
1_adult		Denys	Netherland	3	39.64 (10.3	35.26 (9.17	44	26	25	31	56	30	27.48276	29	6.367443	18.16667	30	6.475861	0.032258	31	0.451613	31
1_adult		Kwon	Republic of	3	26.26 (6.9)	26.7 (7.28)	61	62	89	90	179	90	26.66667	90	6.606092	19.04444	90	6.463225	0.011111	90	0.022222	90
1_adult		Benedetti	Italy	3	33.98 (12.3	35.02 (10.3	73	71	62	66	128	66	30.89394	66	5.563974	16.01515	66	6.059938	0.015152	66	0.106061	66
1_adult		Hirano	Japan	3	30.95 (8.36	33.11 (7.82	45	36	44	47	91	47	26.29787	47	3.838676	22.74468	47	7.971329	0.085106	47	0.170213	47
1_adult		Koch	Germany	3	30.27 (9.04	30.91 (9.55	39	37	74	76	150	76	20.77333	75	6.079592	16.97222	72	6.7427	0	0	0	0
1_adult		Stein	South-Afric	3	30.59 (10.7	30.48 (10.6	38	48	29	23	52	23	23.08696	23	4.144142	14	23	6.775625	0	23	0	23
1_adult		Tolin	USA	3	48 (11.87)	32.11 (12.0	22	67	32	27	59	25	22.74074	27	4.760354	NA	0	NA	0.444444	27	0.407407	27
1_adult		Simpson	USA	3	28.27 (8.04	29.62 (7.98	52	52	33	33	66	33	25.54545	33	3.691975	15.0303	33	7.042216	0.212121	33	0.30303	33
1_adult		Nakao	Japan	3	39.34 (12.9	36.6 (10.02	39	42	41	81	122	81	22.48052	77	5.609227	24.61728	81	9.466478	0	0	0.358025	72
1_adult		Spalletta	Italy	3	36.52 (10.5	36.67 (11.5	59	67	128	84	212	79	23.4375	80	8.99767	18.90123	81	10.922	0.095238	83	0.095238	83
1_adult		Stern	USA	3	28.17 (7.15	27.87 (6.9)	44	33	18	15	33	15	18.8	15	4.161044	12.4	15	5.877317	0.466667	15	0.133333	15
1_adult		Wang	China	3	26.24 (7.55	29.47 (9.33	54	55	37	53	90	53	25.33962	53	5.003627	23.18868	53	10.41644	0	53	0	53
1_adult		Nurmi	USA	3	30.76 (11.7	33.31 (11.0	56	51	25	49	74	48	24.61224	49	4.334053	10.85417	48	4.345404	0.346939	48	0.183673	48
1_adult		Walitza	Switzerland	3	32.89 (9.21	30.72 (7.76	28	47	18	17	35	16	17.11765	17	9.942851	16.71429	14	7.79969	0.470588	16	0.470588	16
1_adult		Reddy	India	3	26.59 (4.88	29.5 (6.74)	64	53	170	203	373	203	25.87192	203	6.289497	22.08867	203	7.58725	0.073892	203	0.152709	203

Asy	Estimate	SE	tvalue	Chisq	ChiDf	pval	modelKapp	MaxVIF	Nobs	Ngrp	Cohensd
Asy_LatVer	-0.0063	0.01911	-0.3299	0.108434	1	0.741934	9.857069	1.011682	907	16	-0.02178
Asy_thal	0.010833	0.003818	2.837204	8.010514	1	0.004651	9.85345	1.012242	874	16	0.187314
Asy_caud	-0.00462	0.00368	-1.25456	1.571685	1	0.209963	9.929375	1.00766	877	16	-0.08283
Asy_put	-0.00253	0.00438	-0.57663	0.332405	1	0.564247	9.728497	1.010341	854	16	-0.03807
Asy_pal	-0.02439	0.007687	-3.17271	9.998788	1	0.001566	9.687887	1.010574	803	16	-0.20946
Asy_hippo	-0.00453	0.005691	-0.79659	0.631577	1	0.426777	9.98058	1.012132	880	16	-0.05259
Asy_amyg	0.002868	0.007929	0.361693	0.130785	1	0.71762	10.05577	1.011015	836	16	0.023879
Asy_accum	0.012355	0.010246	1.205911	1.452763	1	0.228085	9.878027	1.009809	884	16	0.079615

Asy	Estimate	SE	tvalue	Chisq	ChiDf	pval	modelKapp	MaxVIF	Nobs	Ngrp	Cohensd
Asy_banks	-0.00396	0.005698	-0.69487	0.482662	1	0.487219	10.15751	1.005441	822	16	-0.04576
Asy_caudal	0.00112	0.007332	0.1527	0.023316	1	0.878639	10.08108	1.009679	883	16	0.010056
Asy_caudal	0.004047	0.003817	1.060338	1.123451	1	0.289177	9.914128	1.010459	901	16	0.069827
Asy_cuneu	-0.00157	0.004674	-0.33653	0.112499	1	0.737317	9.945658	1.00989	907	16	-0.02216
Asy_entorh	-0.00193	0.009044	-0.21343	0.045381	1	0.831306	9.940295	1.011281	787	16	-0.01405
Asy_fusifor	-0.00139	0.00313	-0.44361	0.19666	1	0.65743	10.00826	1.010127	894	16	-0.02921
Asy_inferio	-0.00366	0.00322	-1.13773	1.293326	1	0.255436	9.932306	1.010238	857	16	-0.07492
Asy_inferio	0.001606	0.004181	0.384069	0.147486	1	0.70095	10.03775	1.011345	895	16	0.025292
Asy_isthmu	-0.00784	0.005552	-1.41283	1.992334	1	0.158097	10.00024	1.009062	902	16	-0.09304
Asy_lateral	-0.00687	0.003302	-2.08126	4.321256	1	0.037639	10.13388	1.008183	899	16	-0.13706
Asy_lateral	0.002169	0.004131	0.525008	0.275414	1	0.599723	9.984136	1.009805	915	16	0.034574
Asy_lingual	-0.00376	0.003413	-1.10267	1.213328	1	0.270674	9.95034	1.009414	913	16	-0.07261
Asy_media	-0.0066	0.005312	-1.24284	1.542851	1	0.214194	9.995089	1.008689	894	16	-0.08185
Asy_middle	0.001371	0.003943	0.34779	0.120903	1	0.728057	9.941047	1.008475	863	16	0.022903
Asy_parahi	0.007026	0.006579	1.067873	1.132033	1	0.287342	9.964504	1.010479	891	16	0.070323
Asy_parace	-0.0012	0.003632	-0.32921	0.108118	1	0.742298	9.932681	1.009699	910	16	-0.02168
Asy_parsop	0.001335	0.004201	0.317709	0.100884	1	0.750771	9.999529	1.009139	896	16	0.020922
Asy_parsor	-0.00404	0.006612	-0.61105	0.37262	1	0.54158	9.973953	1.010218	911	16	-0.04024
Asy_parstri	0.003975	0.004659	0.853124	0.727043	1	0.393843	9.975982	1.008743	909	16	0.056181
Asy_perica	-0.00523	0.005254	-0.99495	0.986119	1	0.320693	9.942551	1.008402	907	16	-0.06552
Asy_postce	0.001675	0.003408	0.49152	0.241518	1	0.623112	9.865235	1.010055	876	16	0.032368
Asy_poster	-0.00099	0.004329	-0.22881	0.05235	1	0.819024	10.01366	1.009695	903	16	-0.01507
Asy_precer	0.0023	0.002847	0.807927	0.652319	1	0.419285	9.969332	1.010921	884	16	0.053205
Asy_precur	-0.00304	0.002815	-1.07933	1.164028	1	0.280632	9.98606	1.009357	908	16	-0.07108
Asy_rostral	0.00741	0.006479	1.143778	1.304816	1	0.253335	10.12114	1.007834	879	16	0.075322
Asy_rostral	0.001656	0.003541	0.467796	0.218746	1	0.639997	9.924277	1.009199	910	16	0.030806
Asy_superi	-0.00158	0.002593	-0.61057	0.37266	1	0.541558	9.988786	1.008948	883	16	-0.04021
Asy_superi	0.002053	0.002618	0.7841	0.614499	1	0.433099	10.0552	1.010093	901	16	0.051636
Asy_superi	0.003257	0.003392	0.960125	0.921029	1	0.337205	10.12563	1.00681	842	16	0.063227
Asy_suprar	-0.00441	0.003652	-1.20862	1.45942	1	0.227022	10.07103	1.009655	844	16	-0.07959
Asy_fronta	-0.00973	0.00919	-1.05823	1.115013	1	0.290995	9.961991	1.009524	911	16	-0.06969
Asy_tempo	0.002393	0.008466	0.282601	0.079859	1	0.777488	9.978551	1.010806	903	16	0.01861

Asy_transv	-0.00684	0.006466	-1.05746	1.115633	1	0.290861	9.977537	1.008229	910	16	-0.06964
Asy_insula	0.002479	0.003566	0.695157	0.482858	1	0.48713	9.854359	1.008494	878	16	0.045778
Asy_Thickn	-0.00013	0.001139	-0.11325	0.012808	1	0.909893	9.954367	1.009411	921	16	-0.00746

Asy	Estimate	SE	tvalue	Chisq	ChiDf	pval	modelKapp	MaxVIF	Nobs	Ngrp	Cohensd
Asy_banks	-0.01016	0.012033	-0.8447	0.713086	1	0.398421	10.17504	1.005496	819	16	-0.05563
Asy_caudal	-0.01708	0.016022	-1.06631	1.135711	1	0.28656	10.08108	1.010339	883	16	-0.07022
Asy_caudal	-0.00583	0.010253	-0.56882	0.322662	1	0.570012	9.918312	1.010409	900	16	-0.03746
Asy_cuneu	0.008555	0.008994	0.951234	0.904029	1	0.341704	9.944461	1.009852	906	16	0.062642
Asy_entorh	-0.02096	0.017526	-1.19596	1.42844	1	0.232019	9.945843	1.011246	786	16	-0.07876
Asy_fusifor	0.008899	0.0069	1.289724	1.66082	1	0.197493	10.01745	1.009945	894	16	0.084933
Asy_inferio	-0.00487	0.00728	-0.66911	0.447473	1	0.503538	9.945049	1.0102	855	16	-0.04406
Asy_inferio	-0.00332	0.007664	-0.43333	0.186145	1	0.666145	10.03127	1.010757	893	16	-0.02854
Asy_isthmu	0.013572	0.010416	1.303011	1.696225	1	0.192782	10.00914	1.009362	901	16	0.085808
Asy_lateral	0.006456	0.006677	0.966837	0.934289	1	0.333751	10.13388	1.010817	899	16	0.06367
Asy_lateral	-0.0071	0.005801	-1.22326	1.495048	1	0.221435	9.984136	1.009871	915	16	-0.08056
Asy_lingual	0.004649	0.006584	0.706162	0.49786	1	0.480442	9.940009	1.009689	911	16	0.046503
Asy_media	-0.0008	0.008226	-0.09783	0.00957	1	0.92207	9.995089	1.008611	894	16	-0.00644
Asy_middle	-0.00666	0.006379	-1.04467	1.081865	1	0.298281	9.933859	1.009098	862	16	-0.06879
Asy_parahi	0.01364	0.010493	1.299986	1.683169	1	0.194504	9.972792	1.010335	889	16	0.085608
Asy_parace	0.01089	0.009004	1.20947	1.461643	1	0.226669	9.932681	1.012243	910	16	0.079648
Asy_parsop	0.002621	0.010742	0.244039	0.057491	1	0.810506	9.999529	1.00955	896	16	0.016071
Asy_parsor	-0.00095	0.008842	-0.10734	0.011511	1	0.914561	9.973953	1.0103	911	16	-0.00707
Asy_parstri	0.0175	0.010416	1.680083	2.811898	1	0.093568	9.975982	1.009466	909	16	0.110639
Asy_perica	-0.00625	0.007987	-0.78229	0.611579	1	0.434194	9.93031	1.008302	906	16	-0.05152
Asy_postce	-0.00324	0.006661	-0.48713	0.237248	1	0.626201	9.880203	1.00981	876	16	-0.03208
Asy_poster	-0.00629	0.010211	-0.61633	0.3796	1	0.537817	10.02426	1.009778	902	16	-0.04059
Asy_precer	-0.00675	0.005123	-1.31732	1.712211	1	0.190699	9.975064	1.011688	884	16	-0.08675
Asy_precur	-0.00199	0.005613	-0.35535	0.12208	1	0.72679	9.98606	1.010689	908	16	-0.0234
Asy_rostral	-0.01515	0.01423	-1.06465	1.132328	1	0.287279	10.09018	1.008475	880	16	-0.07011
Asy_rostral	-0.00575	0.005594	-1.0282	1.056195	1	0.304085	9.924277	1.010275	910	16	-0.06771
Asy_superi	0.00504	0.004555	1.10665	1.214148	1	0.270512	9.988786	1.010904	883	16	0.072877
Asy_superi	0.00106	0.005905	0.179475	0.032123	1	0.857759	10.0552	1.010637	901	16	0.011819
Asy_superi	0.005293	0.005972	0.88626	0.784916	1	0.375642	10.08724	1.007462	837	16	0.058363
Asy_suprar	0.002744	0.009007	0.304657	0.092791	1	0.760658	10.06199	1.010346	841	16	0.020063
Asy_fronta	-0.02173	0.012362	-1.75741	3.077073	1	0.079403	9.955838	1.009423	911	16	-0.11573
Asy_tempo	0.016321	0.011577	1.40978	1.984868	1	0.158879	9.977947	1.010862	902	16	0.092839

Asy_transv	-0.00256	0.011151	-0.22942	0.05248	1	0.818802	9.977537	1.00821	910	16	-0.01511
Asy_insula	-0.0026	0.006075	-0.42776	0.18296	1	0.668842	9.844243	1.007902	877	16	-0.02817
Asy_SurfAr	0.000895	0.001189	0.752936	0.565673	1	0.451983	9.954367	1.009507	921	16	0.049583

Asy	Estimate	SE	tvalue	Chisq	ChiDf	pval	modelKapp	MaxVIF	Nobs	Ngrp	Cohensd
Asy_LatVer	0.008776	0.008761	1.001739	1.002323	1	0.316749	6.519114	1.006996	3393	30	0.034353
Asy_thal	0.003074	0.002475	1.241878	1.54184	1	0.214344	6.536999	1.004978	3200	30	0.042588
Asy_caud	0.001766	0.002092	0.843837	0.711985	1	0.398786	6.478008	1.005814	3299	30	0.028938
Asy_put	-0.0005	0.002557	-0.19423	0.037708	1	0.84603	6.495542	1.006012	3134	30	-0.00666
Asy_pal	0.008872	0.005072	1.749399	3.058806	1	0.080301	6.492306	1.005229	3083	30	0.059993
Asy_hippo	-0.0038	0.00215	-1.76881	3.127126	1	0.076999	6.472522	1.006001	3319	30	-0.06066
Asy_amyg	-0.00303	0.003693	-0.82074	0.67324	1	0.411924	6.479848	1.005388	3303	30	-0.02815
Asy_accum	-0.01153	0.006031	-1.91201	3.651221	1	0.056028	6.515889	1.005721	3348	30	-0.06557

Asy	Estimate	SE	tvalue	Chisq	ChiDf	pval	modelKapp	MaxVIF	Nobs	Ngrp	Cohensd
Asy_banks	-0.00061	0.002934	-0.20821	0.043352	1	0.835064	6.599419	1.008297	2830	30	-0.00726
Asy_caudal	0.003437	0.004064	0.845685	0.713716	1	0.398213	6.556573	1.007117	3209	30	0.029494
Asy_caudal	-0.00115	0.001835	-0.62496	0.390485	1	0.532045	6.578132	1.00691	3242	30	-0.0218
Asy_cuneu	0.001632	0.002339	0.697553	0.486399	1	0.485538	6.579057	1.007314	3182	30	0.024328
Asy_entorh	-0.0082	0.004516	-1.81521	3.29256	1	0.069594	6.49113	1.007412	2798	30	-0.06331
Asy_fusifor	-0.00054	0.001613	-0.33332	0.111041	1	0.738962	6.523245	1.006473	3229	30	-0.01163
Asy_inferio	0.000647	0.001557	0.415887	0.172897	1	0.67755	6.566631	1.007451	3071	30	0.014505
Asy_inferio	-0.00191	0.001932	-0.98632	0.972302	1	0.324107	6.532027	1.006727	3183	30	-0.0344
Asy_isthmu	-0.00119	0.002842	-0.41909	0.175622	1	0.675163	6.521665	1.006901	3277	30	-0.01462
Asy_lateral	-8.92E-05	0.001648	-0.05411	0.002927	1	0.956851	6.520692	1.006637	3234	30	-0.00189
Asy_lateral	0.000571	0.001944	0.293806	0.086321	1	0.768908	6.552554	1.006511	3283	30	0.010247
Asy_lingual	-0.00092	0.001867	-0.4948	0.244731	1	0.62081	6.541362	1.006303	3272	30	-0.01726
Asy_media	0.000785	0.002421	0.324373	0.105129	1	0.745759	6.537873	1.006549	3260	30	0.011313
Asy_middle	-0.00086	0.001835	-0.46912	0.220061	1	0.638993	6.588218	1.006576	2989	30	-0.01636
Asy_parahi	-0.00033	0.003366	-0.09936	0.00983	1	0.921023	6.541253	1.007087	3249	30	-0.00347
Asy_parace	-0.00182	0.001841	-0.98641	0.972855	1	0.323969	6.543491	1.006626	3274	30	-0.0344
Asy_parsop	-0.00014	0.002122	-0.06527	0.00426	1	0.947961	6.566621	1.007016	3240	30	-0.00228
Asy_parsor	0.001076	0.003085	0.34879	0.121629	1	0.727274	6.544614	1.007491	3274	30	0.012164
Asy_parstri	0.002345	0.002233	1.050074	1.102063	1	0.293814	6.545042	1.006376	3236	30	0.036622
Asy_perica	-0.00186	0.00268	-0.69454	0.482021	1	0.487508	6.579378	1.006447	3213	30	-0.02422
Asy_postce	-0.00343	0.001637	-2.09513	4.386527	1	0.036224	6.568952	1.008696	3183	30	-0.07307
Asy_poster	-0.00299	0.002197	-1.36244	1.855697	1	0.173122	6.538804	1.006767	3268	30	-0.04752
Asy_precer	3.38E-05	0.00147	0.023014	0.000529	1	0.981643	6.579372	1.007019	3175	30	0.000803
Asy_precur	0.000171	0.001439	0.119066	0.014176	1	0.905224	6.53858	1.006427	3268	30	0.004153
Asy_rostral	-0.00609	0.003373	-1.80539	3.248716	1	0.071479	6.563661	1.006129	3197	30	-0.06296
Asy_rostral	-0.00061	0.001511	-0.40395	0.16312	1	0.6863	6.552892	1.006029	3259	30	-0.01409
Asy_superi	-0.00119	0.001088	-1.09798	1.205156	1	0.272294	6.540721	1.006556	3160	30	-0.03829
Asy_superi	-0.00014	0.001252	-0.11216	0.012579	1	0.9107	6.539568	1.007226	3205	30	-0.00391
Asy_superi	9.18E-05	0.00172	0.053341	0.002845	1	0.957461	6.593004	1.006111	2801	30	0.00186
Asy_suprar	-0.00194	0.001722	-1.1261	1.267778	1	0.260184	6.615561	1.007538	2863	30	-0.03927
Asy_fronta	-0.00492	0.004327	-1.13811	1.28527	1	0.256922	6.533115	1.007892	3279	30	-0.03969
Asy_tempo	0.003824	0.003793	1.008105	1.016082	1	0.31345	6.519806	1.006194	3246	30	0.035159

Asy_transv	0.001634	0.003393	0.481524	0.231837	1	0.630165	6.553961	1.009711	3282	30	0.016794
Asy_insula	-0.00065	0.001748	-0.3698	0.136747	1	0.711537	6.562418	1.006633	3195	30	-0.0129
Asy_Thickn	-0.0005	0.000549	-0.91344	0.833926	1	0.36114	6.539374	1.006995	3288	30	-0.03186

Asy	Estimate	SE	tvalue	Chisq	ChiDf	pval	modelKapp	MaxVIF	Nobs	Ngrp	Cohensd
Asy_banks	-0.00237	0.00578	-0.41004	0.168123	1	0.681785	6.598265	1.009983	2825	30	-0.0143
Asy_caudal	0.012354	0.008658	1.426878	2.027754	1	0.154449	6.556573	1.009838	3209	30	0.049764
Asy_caudal	-0.00139	0.00522	-0.26613	0.070525	1	0.790573	6.578132	1.008447	3242	30	-0.00928
Asy_cuneu	0.002542	0.004435	0.573159	0.328491	1	0.566549	6.579057	1.007564	3182	30	0.01999
Asy_entorh	0.00052	0.008666	0.059958	0.003595	1	0.952191	6.485991	1.007691	2795	30	0.002091
Asy_fusifor	0.002167	0.003609	0.600342	0.352807	1	0.552528	6.523245	1.008521	3229	30	0.020938
Asy_inferio	-0.0021	0.003671	-0.57315	0.328167	1	0.56674	6.558291	1.008405	3069	30	-0.01999
Asy_inferio	-0.00487	0.004062	-1.19896	1.435216	1	0.230915	6.532027	1.008021	3183	30	-0.04181
Asy_isthmu	0.001208	0.005114	0.236135	0.055743	1	0.813356	6.521665	1.007514	3277	30	0.008235
Asy_lateral	-0.00117	0.003408	-0.34439	0.1186	1	0.730557	6.520692	1.009953	3234	30	-0.01201
Asy_lateral	-0.00274	0.002652	-1.0337	1.068291	1	0.301332	6.552554	1.006652	3283	30	-0.03605
Asy_lingual	-0.00167	0.003539	-0.47167	0.222246	1	0.637334	6.541362	1.006668	3272	30	-0.01645
Asy_media	-0.00276	0.00393	-0.70257	0.493564	1	0.482342	6.537873	1.006608	3260	30	-0.0245
Asy_middle	0.003865	0.003274	1.180436	1.393105	1	0.237881	6.58786	1.008325	2988	30	0.041169
Asy_parahi	0.00219	0.00473	0.462913	0.21416	1	0.643526	6.542536	1.008238	3249	30	0.016145
Asy_parace	-0.00525	0.004518	-1.16261	1.349825	1	0.245309	6.543491	1.009328	3274	30	-0.04055
Asy_parsop	-0.00486	0.005671	-0.85649	0.730894	1	0.392594	6.566621	1.008865	3240	30	-0.02987
Asy_parsor	-0.00319	0.004275	-0.74672	0.553486	1	0.456897	6.544614	1.008852	3274	30	-0.02604
Asy_parstri	-0.00635	0.005128	-1.23749	1.526421	1	0.21665	6.545042	1.008077	3236	30	-0.04316
Asy_perica	0.002941	0.003994	0.736326	0.541984	1	0.461612	6.579378	1.006423	3213	30	0.02568
Asy_postce	-0.00684	0.003226	-2.11924	4.480988	1	0.034274	6.568276	1.009736	3180	30	-0.07391
Asy_poster	0.007827	0.005261	1.487809	2.210368	1	0.137086	6.538804	1.009191	3268	30	0.051889
Asy_precer	-0.00061	0.00285	-0.21307	0.045314	1	0.831428	6.579127	1.008675	3173	30	-0.00743
Asy_precur	0.003155	0.002744	1.14972	1.319884	1	0.250613	6.53858	1.00883	3268	30	0.040098
Asy_rostral	0.010981	0.007568	1.450937	2.103009	1	0.14701	6.563661	1.009235	3197	30	0.050603
Asy_rostral	-0.00271	0.002769	-0.97838	0.955859	1	0.328232	6.552892	1.007681	3259	30	-0.03412
Asy_superi	-0.00173	0.002427	-0.71115	0.5048	1	0.477399	6.540721	1.010053	3160	30	-0.0248
Asy_superi	-0.00013	0.003136	-0.04091	0.001674	1	0.967369	6.539568	1.009122	3205	30	-0.00143
Asy_superi	0.000359	0.002924	0.122767	0.014942	1	0.902712	6.589159	1.008673	2792	30	0.004282
Asy_suprar	-0.00043	0.004441	-0.09768	0.009531	1	0.922227	6.610771	1.009265	2855	30	-0.00341
Asy_fronta	-0.00839	0.006484	-1.29479	1.67309	1	0.195845	6.533115	1.008282	3279	30	-0.04516
Asy_tempo	-0.00495	0.005547	-0.89249	0.796297	1	0.372203	6.519806	1.00683	3246	30	-0.03113

Asy_transv	-0.00945	0.005574	-1.69461	2.870415	1	0.090222	6.553961	1.007473	3282	30	-0.0591
Asy_insula	-0.00131	0.002965	-0.44325	0.196417	1	0.657628	6.566534	1.00665	3200	30	-0.01546
Asy_SurfAr	-0.00127	0.000513	-2.47964	6.125434	1	0.013325	6.542183	1.007607	3291	30	-0.08648